bioRxiv preprint doi: https://doi.org/10.1101/2021.04.09.439146; this version posted April 9, 2021. The copyright holder for this preprint (which was not certified by peer review) is the author/funder, who has granted bioRxiv a license to display the preprint in perpetuity. It is made available under aCC-BY 4.0 International license.

Full title:

Herpes simplex virus 2 (HSV-2) evolves faster in cell culture than HSV-1 by generating greater genetic diversity

Short title:

Differential *in vitro* generation of genetic diversity of HSV

Alberto Domingo López-Muñoz[1,#a], Alberto Rastrojo[1,#b], Rocío Martín[1], Antonio Alcamí[1]*

[1] Centro de Biología Molecular Severo Ochoa (Consejo Superior de Investigaciones Científicas and Universidad Autónoma de Madrid), Madrid, Spain

[#a]Current address: Cellular Biology Section, Laboratory of Viral Diseases, NIAID, NIH, United States

[#b]Current address: Genetic Unit, Department of Biology, Universidad Autónoma de Madrid, Madrid, Spain

* Corresponding author

E-mail: aalcami@cbm.csic.es

bioRxiv preprint doi: https://doi.org/10.1101/2021.04.09.439146; this version posted April 9, 2021. The copyright holder for this preprint (which was not certified by peer review) is the author/funder, who has granted bioRxiv a license to display the preprint in perpetuity. It is made available under aCC-BY 4.0 International license.

ABSTRACT

Herpes simplex virus type 1 and 2 (HSV-1 and HSV-2, respectively) are prevalent human pathogens of clinical relevance that establish long-life latency in the nervous system. They have been considered, along with the *Herpesviridae* family, to exhibit a low level of genetic diversity during viral replication. However, the high ability shown by these viruses to rapidly evolve under different selective pressures does not correlates with that presumed genetic stability. High-throughput sequencing has revealed that heterogeneous or plaque-purified populations of both serotypes contain a broad range of genetic diversity, in terms of number and frequency of minor genetic variants, both *in vivo* and *in vitro*. This is reminiscent of the quasispecies phenomenon traditionally associated with RNA viruses. Here, by plaque-purification of two selected viral clones of each viral subtype, we reduced the high level of genetic variability found in the original viral stocks, to more genetically homogeneous populations. After having deeply characterized the genetic diversity present in the purified viral clones as a high confidence baseline, we examined the generation of *de novo* genetic diversity under culture conditions. We found that both serotypes gradually increased the number of *de novo* minor variants, as well as their frequency, in two different cell types after just five and ten passages. Remarkably, HSV-2 populations displayed a much higher raise of nonconservative *de novo* minor variants than the HSV-1 counterparts. Most of these minor variants exhibited a very low frequency in the population, increasing their frequency over sequential passages. These new appeared minor variants largely impacted the coding diversity of HSV-2, and we found some genes more prone to harbor higher variability. These data show that herpesviruses generate *de novo* genetic diversity differentially under equal *in vitro* culture conditions. This might have contributed to the evolutionary divergence of HSV-1 and HSV-2 adapting to different anatomical niche, boosted by selective pressures found at each epithelial and neuronal tissue.

bioRxiv preprint doi: https://doi.org/10.1101/2021.04.09.439146; this version posted April 9, 2021. The copyright holder for this preprint (which was not certified by peer review) is the author/funder, who has granted bioRxiv a license to display the preprint in perpetuity. It is made available under aCC-BY 4.0 International license.

AUTHOR SUMMARY

Herpesviruses are highly human pathogens that establish latency in neurons of the peripheral nervous system. Colonization of nerve endings is required for herpes simplex virus (HSV) persistence and pathogenesis. HSV-1 global prevalence is much higher than HSV-2, in addition to their preferential tendency to infect the oronasal and genital areas, respectively. How these closely related viruses have been adapting and evolving to replicate and colonize these two different anatomical areas remains unclear. Herpesviruses were presumed to mutate much less than viruses with RNA genomes, due to the higher fidelity of the DNA polymerase and proofreading mechanisms when replicating. However, the worldwide accessibility and development of high-throughput sequencing technologies have revealed the heterogenicity and high diversity present in viral populations clinically isolated. Here we show that HSV-2 mutates much faster than HSV-1, when compared under similar and controlled cell culture conditions. This high mutation rate is translated into an increase in coding diversity, since the great majority of these new mutations lead to nonconservative changes in viral proteins. Understanding how herpesviruses differentially mutate under similar selective pressures is critical to prevent resistance to anti-viral drugs.

bioRxiv preprint doi: https://doi.org/10.1101/2021.04.09.439146; this version posted April 9, 2021. The copyright holder for this preprint (which was not certified by peer review) is the author/funder, who has granted bioRxiv a license to display the preprint in perpetuity. It is made available under aCC-BY 4.0 International license.

INTRODUCTION

Herpes simplex virus (HSV) is well-known for being one of the most prevalent neurotropic pathogens worldwide, causing a broad range of diseases in humans. The latest epidemiological studies estimate around 66% and 13.2% of global seroprevalence for HSV-1 and HSV-2, respectively, depending on age, sex, and geographical region [1]. HSV-1 infects the oral mucosa preferentially, causing characteristic minor skin lesions and eventually, encephalitis. Genital herpes is more often caused by HSV-2. Nevertheless, both viruses can infect either mucosa, frequently as a consequence of oral-genital sex [2-5]. After initial replication and dissemination at epithelial tissue, HSV infects sensory neuronal endings innervating the tissue [6, 7]. Once the virus reaches the trigeminal ganglia or the dorsal root ganglia, the virus establishes latency for the host's lifetime. The virus periodically reactivates from latent to replicative stage, traveling anterogradely back to the epithelial tissue, where recurrent infection and transmission occur, exhibiting associated disease symptoms [8]. During these multiple cycles of latency and reactivation, the virus may reinfect the nervous system or be transmitted to a new host, finding numerous chances to expand its genetic repertoire for subsequent reactivation cycles [9, 10]. The genetic diversity of the reactivating viral population can evolve by genetic drift, allowing the virus to respond to the host selective pressures that it faces when replicating. Other than the selective pressures due to immunological surveillance at the replication site, the virus may undergo selection in response to the differences between epithelial and neuronal environments [11-13]. Since HSV-1 and HSV-2 exhibit a preference for infecting different anatomical areas, it is reasonable to think that the selective pressures during each cycle of latency and reactivation might have contributed differentially to their evolution in humans, adapting their life cycle to each epithelial and neuronal niche.

The HSV genome is 152-155 Kilobase pairs long of double-stranded DNA, varying slightly between subtypes and strains. The genome is organized as unique long (UL)

bioRxiv preprint doi: https://doi.org/10.1101/2021.04.09.439146; this version posted April 9, 2021. The copyright holder for this preprint (which was not certified by peer review) is the author/funder, who has granted bioRxiv a license to display the preprint in perpetuity. It is made available under aCC-BY 4.0 International license.

and unique short (US) coding regions, flanked by terminal/internal long/short structural repeats (i.e., T/I-Repeat(R)-L/S). The “a” sequence is present at the IRL-IRS border, but also at the termini of the TRL and TRS, enabling the inversion of the unique fragments orientation and producing four genomic isomers in equal ratios and functionality [14, 15]. Genomic replication generates long concatemers of viral DNA, which are processed into unit-length genomes after cellular endonuclease G cleavage in the “a” sequence [16]. Those concatemers are highly branched, promoting recombination events between repeated regions and resulting in the inversion of the UL and US segments [17]. Interestingly, high recombination and inversion rates in the HSV genome have been extensively described, assisted by repetitive regions with a high G + C content [18-20]. Fluctuations in copy number, tandem repeats, and homopolymeric areas have been described as a frequent source of genetic variability in HSV-1 [21]. These mechanisms are critical components in the generation of variability within the large structural repeats of the HSV genome, which in fact contain immediate-early expressed genes essential to productive replication [8]. Nonetheless, genetic variability can be generated by different mechanisms other than recombination and copy number/length fluctuations, where genetic drift driven by polymerase error plays a critical role. Misincorporation of nucleotides during genome replication leads to the appearance of single nucleotide polymorphisms (SNPs) and insertions/deletions (InDels) both *in vivo* and *in vitro*. Previous studies proposed a very low mutation rate for HSV-1 polymerase (1×10^{-7} to 1×10^{-8} mutations per base per infectious cycle), despite being performed on a single gene analysis located at a unique coding region [11, 22, 23]. However, that mutation rate does not correlate with the rapid ability observed when selecting HSV variants under drug pressures, either by selection of preexisting minor variants (MVs) in the population or by *de novo* mutations [22, 24-27].

Herpesviruses were presumed to generate lower genetic diversity when replicating and then evolve with a slower rate than RNA viruses, due to their relatively more stable DNA genome and proofreading mechanisms [12, 28, 29]. However, over the last decade, the

bioRxiv preprint doi: https://doi.org/10.1101/2021.04.09.439146; this version posted April 9, 2021. The copyright holder for this preprint (which was not certified by peer review) is the author/funder, who has granted bioRxiv a license to display the preprint in perpetuity. It is made available under aCC-BY 4.0 International license.

idea that herpesviruses exist as heterogenic and highly diverse populations *in vivo* has gained increasing supportive evidence, aided by worldwide accessibility and cost reduction of high-throughput sequencing technologies [30-33]. Nonetheless, how this increasingly evident generation of genetic variability is generated remains not well characterized. Shipley et al. reported that the genetic diversity of HSV-1 is able to change over multiple cycles of latency and reactivation in the genital context [34]. Clinical isolates of HSV-2 from a neonatal population showed extensive intra-host diversity, displaying different *in vitro* phenotypes [31]. A similar level of generation of genetic diversity may happen *in vitro* as well, where the method of preparation/propagation of HSV stocks plays a key role [35]. In this context, multiple rounds of amplification in cell culture increase the heterogenicity of viral stocks by genetic drift, where plaque-isolation has been classically used to reduce the impact of this evolutionary force. HSV has been routinely propagated in African green monkey kidney (Vero) cells, which are interferon incompetent [36]. This, together with the fact that these cells are not of human origin and just represent only one cell type among all the ones that HSV faces when infecting humans, very likely impact the generation of genetic diversity *in vitro*. On the other hand, *in vitro* studies of viral evolution can bring an ideal scenario with more controlled and reduced selective pressures, where gaining insights into the mechanisms governing the generation of genetic variability can be easier. Kuny et al. [37] have recently reported that a heterogeneous population of HSV-1 increased its genetic diversity and changed its phenotype more dramatically than a plaque-purified population of the same strain, after ten passages in Vero cells. Certain genetic MVs already present in the heterogeneous population appeared to be positively selected, whereas the purified population did not appear to increase its MVs repertoire. However, the number and frequency of the *de novo* mutations that appeared over those ten sequential passages in Vero cells were not assessed. As far as we know, similar studies reporting how HSV-2 *in vitro* evolves in terms of generation of genetic diversity have not been reported yet. Thus, how differentially fast this genetic diversity is *de novo* generated *in vitro*, and how

bioRxiv preprint doi: https://doi.org/10.1101/2021.04.09.439146; this version posted April 9, 2021. The copyright holder for this preprint (which was not certified by peer review) is the author/funder, who has granted bioRxiv a license to display the preprint in perpetuity. It is made available under aCC-BY 4.0 International license.

it impacts the potential coding diversity (and thus, evolution) between HSV-1 and HSV-2, remains unclear.

Here we performed sequential passage of two plaque-purified populations of both HSV-1 and HSV-2 to characterize the differential ability and speed of these closely related viruses to *in vitro* evolve in two different cell lines. We first assessed the genetic diversity present in our original viral stocks by high-throughput sequencing, isolating plaque-purified clones, and sequencing them. After nonconservative variant analysis, two purified clones were ultra-deep re-sequenced, characterized in cell culture, and tested in animal models of infection; in order to ensure that the genetic bottleneck of the plaque-purification procedure did not alter the viral infectiousness due to a deleterious variant unintentionally selected [38-40]. After establishing a high confident baseline of the genetic diversity present in each purified population at passage 0 (P0), each of them was subjected to ten serial passages in Vero and HaCaT cells, and ultra-deep sequenced at passage 5 (P5) and passage 10 (P10). We detected the frequency and distribution of preexisting and *de novo* genetic MVs, examining their impact on the coding capacity of both HSV serotypes. These results have helped us to better understand how each HSV subtype differentially evolves, depending on the selective pressures behind a given cellular environment, and brings new insights into the different generation of genetic diversity of the closely related HSV-1 and HSV-2.

bioRxiv preprint doi: https://doi.org/10.1101/2021.04.09.439146; this version posted April 9, 2021. The copyright holder for this preprint (which was not certified by peer review) is the author/funder, who has granted bioRxiv a license to display the preprint in perpetuity. It is made available under aCC-BY 4.0 International license.

RESULTS

The viral phenotype of plaque-purified clones may dramatically change just in ten passages in cell culture

To better understand the generation of genetic diversity in HSV-1 and HSV-2, we first isolated five viral clones from both HSV-1 strain SC16 and HSV-2 strain 333 original stocks after five rounds of sequential plaque purification in Vero cells (Fig 1A). This was done in order to reduce the preexisting genetic variability present in the original viral populations, which was used as the baseline to assess the generation of genetic variability.

Both original stock and purified clones, for each serotype, were deep-sequenced (S1-S3 Figs, see S1 Table for genome sequence statistics). After variant analysis, two purified clones for each subtype were selected: clones 2 and 3 for HSV-1, and clones 1 and 5 for HSV-2. This selection was based on the lowest degree of nonconservative variability compared to their corresponding reference sequence, previously described as *de novo* assembled consensus genomes of the same original stocks used in this study [41, 42]. We compared the virus growth kinetics in cell culture, as well as the infectivity and pathogenesis of these selected purified clones to their parental populations in mouse models of infection, in order to ensure that the MVs detected in the purified populations did not affect its viral fitness significantly (S4 Fig and S1 Text). These selected purified clones were then ultra-deep re-sequenced (referred to as P0, Fig 1A), allowing us to accurately identify very low frequency MVs present in these purified populations (S5 Fig). That was a critical step to establish a high confidence baseline in order to be able to discriminate between preexisting or *de novo* generated MVs, due to the intrinsic variability generation rate in each HSV serotype replication cycle.

Each purified clone was used to infect a separate monolayer of Vero and HaCaT cells at a multiplicity of infection (MOI) of 0.1 PFU/cell. Once cytopathic effect was observed, cells and supernatant were harvested. This cycle of infection is considered as a passage

bioRxiv preprint doi: https://doi.org/10.1101/2021.04.09.439146; this version posted April 9, 2021. The copyright holder for this preprint (which was not certified by peer review) is the author/funder, who has granted bioRxiv a license to display the preprint in perpetuity. It is made available under aCC-BY 4.0 International license.

in the generation of variability experiments. The viral stock from the first passages of each selected purified clone was used to infect the next monolayer of Vero and HaCaT cells at the same estimated MOI, being this process repeated for ten sequential passages (Fig 1A, lower part). The viral population of each purified clone in each cell line was ultra-deep sequenced after five and finally ten sequential passages (S6-S9 Figs). An MOI of 0.1 PFU/cell was selected to allow for multiple rounds of replication in each passage, favoring the generation of genetic variability in the viral population.

Kuny et al. [37] did not find any changes in plaque phenotype in an HSV-1 purified population passaged ten times in Vero cells. However, we observed dramatic changes in plaque morphology in the purified HSV-1 clone 3 after ten passages in Vero cells (Fig 1B). After ultra-deep sequencing and variant analysis, we found a nonsynonymous SNP previously described as the cause of the syncytial plaque phenotype [43-45]. The frequency of the R858H variant in the UL27 gene (encoding glycoprotein B, gB) was inexistent at P0 and P5, reaching 46.52% at P10, just in 5 passages in Vero cells (S9 Table, variant #38). In addition, the purified HSV-2 clone 1 also exhibited the same variant at P5 in Vero cells, with a frequency of 1.75% and being undetected at P0 (S11 Table, variant #64). In contrast with HSV-1 clone 3, the frequency of this variant did not increase at P10 for HSV-2 clone 1, not acquiring the syncytial plaque phenotype. Neither this variant nor other syncytia-inducing MVs in gB, such as L817P [37], were detected when purified clones were passaged in HaCaT cells, for both HSV subtypes. These results suggested that even low genetically diverse purified viral populations are able to quickly change or evolve just in a few passages in cell culture, being more prone to happen in some cell lines than in others.

The high genetic diversity found in HSV-1 and HSV-2 original stocks was significantly reduced in five rounds of plaque isolation in Vero cells

Genetic diversity can be defined as nucleotide alleles or variants present in a given percent of the sequencing reads, at a given locus in a sequenced viral population. With

bioRxiv preprint doi: https://doi.org/10.1101/2021.04.09.439146; this version posted April 9, 2021. The copyright holder for this preprint (which was not certified by peer review) is the author/funder, who has granted bioRxiv a license to display the preprint in perpetuity. It is made available under aCC-BY 4.0 International license.

253 enough deep sequencing coverage, these MVs can be confidently detected, revealing
254 the genetic diversity present in the viral population. HSV-1 and HSV-2 original stocks
255 had an average coverage depth of 1783 and 1320 reads/position, respectively (S1
256 Table). We identified SNPs and InDels that were present in greater than 1 percent of the
257 sequencing reads (1 percent cut-off as the threshold of detection, plus additional
258 coverage-dependent filters, see “Material and methods” for detailed criteria). Both viral
259 populations from original stocks had MVs at different sites and frequencies, being evenly
260 distributed across highly repetitive areas and coding regions into their reference genome
261 (S1 Fig). As previously described for other mixed populations of HSV [31, 37], both HSV-
262 1 and HSV-2 original stocks displayed a significant number of MVs (Fig 2A), when
263 sequencing reads were aligned to each corresponding reference genome (*de novo*
264 assembled consensus genome of a purified clone from each same parental stock [41,
265 42]). HSV-1 original stock registered a total of 712 MVs, whereas HSV-2 stock, 1044
266 (Fig 2A, see S3 and S4 Tables for full list). Detailed analysis after variant calling showed
267 that the higher fraction of MVs corresponded to nonsynonymous SNPs for both HSV-1
268 and HSV-2, accounting for 452 and 701, respectively (S2 Table). In terms of frequency,
269 the major fraction of total detected MVs showed to be between 1% - 10% for both HSV
270 serotypes (Fig 2B).
271 Because we found a high level of genetic variability in sequenced viral population from
272 each original stock, we plaque-purified five viral clones from each parental stock in order
273 to use low genetically diverse viral populations as a baseline to evaluate the generation
274 of *de novo* variability in both HSV subtypes. After sequential plaque-isolation of
275 independent viral clones from their parental stocks, sequencing data from these purified
276 viral populations revealed a significant reduction in the number of total detected MVs, for
277 both HSV-1 and HSV-2 (Fig 2C, see S3 and S4 Tables for full list). In fact, every purified
278 clone showed a significant reduction in the total number of MVs, proportionally reflected
279 in the number of nonsynonymous SNPs, for both serotypes. With the exception of HSV-
280 1 clone 4, as well as HSV-2 clone 3, every other purified clone reduced its genetic

bioRxiv preprint doi: https://doi.org/10.1101/2021.04.09.439146; this version posted April 9, 2021. The copyright holder for this preprint (which was not certified by peer review) is the author/funder, who has granted bioRxiv a license to display the preprint in perpetuity. It is made available under aCC-BY 4.0 International license.

variability by 10-fold or higher, when the total detected number of MVs was compared to the number registered for their original stocks. The total number of MVs detected from each clone was grouped by HSV subtype and compared between them, showing no statistically significant differences (Fig 2D), despite the differences in average coverage depth among them (S1 Table). Based on the lowest number of nonconservative changes (i.e., nonsynonymous SNPs and InDels in coding regions) observed among the five purified clones for each HSV subtype, as well as their frequencies in the viral populations, two purified clones of each serotype were selected for further characterization and *in vitro* evolution studies. HSV-1 clones 2 and 3 were selected and tracked by a differential SNP in the UL14 CDS (#162, S3 Table), while HSV-2 clones 1 and 5, by a differential SNP in the UL13 CDS (#180, S4 Table).

The selected purified clones were used to perform replication kinetics in Vero cells, as well as to infect mice as described in S1 Text, in order to confirm whether the MVs detected could cause a deleterious effect in terms of infectivity and pathogenesis, compared to their parental stocks (S4 Fig). No significant differences were found in the replication and infectivity of the purified clones (S4A Fig). Despite finding some variability in terms of survival when compared to original stocks, all four selected clones were able to successfully infect and cause disease in both mouse models of infection tested (S4B Fig), understanding that none of the unintentionally selected MVs during the plaque-purification genetic bottleneck caused a significant deleterious effect. Thus, plaque-isolation proved to be a successful approach to decrease the genetic diversity in the purified viral populations before studying the generation of genetic variability in cell culture. These purified viral populations of more uniformed genetic diversity constituted the key starting point to determine with high confidence the generation of genetic variability, particularly in terms of very low frequency MVs.

bioRxiv preprint doi: https://doi.org/10.1101/2021.04.09.439146; this version posted April 9, 2021. The copyright holder for this preprint (which was not certified by peer review) is the author/funder, who has granted bioRxiv a license to display the preprint in perpetuity. It is made available under aCC-BY 4.0 International license.

Depth of sequencing is critical to establish a high confidence baseline in order to detect very low frequency genetic diversity

Depth of sequencing coverage is instrumental in detecting MVs with high reliance and accuracy. Because the number of sequencing reads correlates directly with the frequency of alleles in the viral population, a higher depth of coverage allows a better resolution of the genetic diversity present in a given viral population. Notably, when identifying *de novo* appeared MVs, a high depth of coverage is crucial to detect the genetic diversity represented with a very low frequency in the viral population (i.e., theoretically at least an average coverage of 200 reads/position, a hundred paired-end reads, would be required in order to be able to detect a 1 percent frequency variant, supported by two reads contained the same allele).

Nonetheless, having an average coverage depth of 200X from a sequenced viral stock containing 10^6 PFU, it would only represent 0.02 percent of the viral population. To surmount the fact that the sequencing of a minute fraction of the whole viral population might seriously bias our ability to detect a given variant, and therefore to determine its novelty, we ultra-deep re-sequenced the previously selected purified viral clones. The average coverage depth increased approx. 2 logs for each purified viral clone, from 10^2 (standard-deep sequencing, SDS) to 10^4 (ultra-deep sequencing, UDS) (Fig 3A, S1 Table). In this context, this depth of coverage would represent a theoretical 1 percent of the viral population (assuming 10^6 PFU), having increased a hundred times the actual genetic diversity sampled from each viral population. Based on this, we understood this level of coverage depth constituted a high confidence representation of the genetic diversity present in each viral population.

A more detailed look at the sequencing statistics of the ten purified clones aforementioned showed that among each serotype, HSV-1 clone 4 and HSV-2 clone 3 showed the highest depth of average coverage, as well as the highest number of total MVs (Fig 2C, S1 Table). This could reasonably lead to think that the lower number of detected MVs in the selected purified clones was due to their lower average coverage.

bioRxiv preprint doi: https://doi.org/10.1101/2021.04.09.439146; this version posted April 9, 2021. The copyright holder for this preprint (which was not certified by peer review) is the author/funder, who has granted bioRxiv a license to display the preprint in perpetuity. It is made available under aCC-BY 4.0 International license.

Nevertheless, we did not find a dramatic increment in the total number of MVs obtained from SDS versus UDS for any of the four selected purified viral clones (Fig 3B, S2 Table). The total number of MVs from SDS versus UDS were grouped and compared, showing no statistically significant differences (Fig 3C left graph), while grouped preexisting MVs did (Fig 3C center graph). The number of preexisting MVs (i.e., variants already detected in the original parental stock) increased in HSV-1 purified clones, being this increment higher in HSV-2 clones (Fig 3B). However, when *de novo* MVs were grouped, there was no statistically significant difference between them (Fig 3C right graph), despite all but HSV-1 clone 3 showing an increment in the total accounted *de novo* MVs (Fig 3B, S2 Table). When we grouped these *de novo* MVs based on their frequency, from SDS versus UDS data, we observed a consistent increase in the number of very low frequency MVs (1% to 2%), as well as a reduction in the number of low frequency MVs (>2% to <10%), across every purified clone (Fig 3D, S2 Table). This reduction in the number of *de novo* low frequency MVs was particularly pronounced in the case of HSV-1 clone 3, explaining the observed decrease in the total number of *de novo* MVs foresaid. Because of the higher depth of average coverage from UDS, we were able to detect a significantly higher number of *de novo* MVs with a very low frequency in the viral populations (Fig 3E), but also to better discriminate the actual frequency of these MVs in the viral population. These improvements of UDS may explain the reduction in the number of low frequency MVs, switching to be detected with a lower frequency when the deep sequencing coverage increases. The fact that the number of preexisting MVs, but not the number of de novo MVs, increased dramatically between SDS vs. UDS indicated that higher depth of coverage helps to gain accuracy and resolution characterizing the existing genetic diversity. Since all four purified clones showed a comparable level of genetic diversity, in terms of total and *de novo* MVs (ranging from 98 to 139, S2 Table), we determined this as a suitable, high confidence starting point to study the generation of genetic variability of both HSV subtypes in cell culture.

bioRxiv preprint doi: https://doi.org/10.1101/2021.04.09.439146; this version posted April 9, 2021. The copyright holder for this preprint (which was not certified by peer review) is the author/funder, who has granted bioRxiv a license to display the preprint in perpetuity. It is made available under aCC-BY 4.0 International license.

HSV-2 *in vitro* evolves dramatically faster than HSV-1 in both Vero and HaCaTs cells

Having characterized the genetic diversity present in each purified viral clone with high confidence, we next investigated how HSV-1 and HSV-2 differentially evolve in cell culture. We conducted ten sequential passages of each purified viral clone separately in Vero and HaCaT cells, ultra-deep sequencing each viral population after 5 and 10 passages in each cell line. We obtained a broad range of average coverage depth, ranging from 872 to 25892 reads/position (S1 Table). Nonhuman primate kidney-derived epithelial (Vero) cells are widely and routinely used for HSV propagation, whereas human keratinocyte (HaCaT) cells are closer to the natural physiology of HSV infection in the skin. HSV plaque formation, cell-to-cell spread, and cell migration were reported to be significantly different when compared HaCaT to Vero cell infections [46]. Based on that, we sought to examine the effects of the differential selective pressures present in each cultured cell line to the generation of genetic diversity of each HSV subtype.

After variant analysis, we analyzed the total number and types of MVs that were present in each viral population at P5 and P10, for every purified clone passaged in each cell type. Most of the detected MVs corresponded to mutations impacting coding regions, including SNPs and InDels (see S2 Table). Nonetheless, both HSV-1 and HSV-2 populations displayed a similar fraction of the total number of MVs impacting coding regions, around 56 percent (+/- 0.094% SD) on average (i.e., nonsynonymous SNPs plus InDels in coding regions, divided by the total number of detected MVs, see S2 Table). We detected a consistently higher total number of MVs among HSV-2 than in HSV-1 viral populations, as well as a higher and increasing number of *de novo* MVs after sequential passages, not previously detected in the purified viral populations at P0 (Fig 4A, S1-S4 Animations). Preexisting variability in HSV-1 populations remained constant over the ten passages in both cell types, but neither a relevant increase in the total number of MVs nor in *de novo* generated MVs were observed (Fig 4A left graph, see S2 Table for more details). However, despite remaining the preexisting number of MVs

bioRxiv preprint doi: https://doi.org/10.1101/2021.04.09.439146; this version posted April 9, 2021. The copyright holder for this preprint (which was not certified by peer review) is the author/funder, who has granted bioRxiv a license to display the preprint in perpetuity. It is made available under aCC-BY 4.0 International license.

392 constant in HSV-2 populations over sequential passages, we found a consistent
393 increment in the appearance of *de novo* generated MVs after five, and even greater,
394 after ten passages for every purified clone (Fig 4A right graph). Both HSV-2 purified
395 clones showed the most drastic increment in the number of *de novo* MVs after being
396 subjected to ten sequential passages in HaCaT cells, dramatically higher than that found
397 when sequentially passaged in Vero cells (Fig 4A right graph). These results showed
398 that HSV-2 generates *de novo* genetic diversity faster than HSV-1, where the selective
399 pressures present in each cell type used for viral propagation may differentially affect
400 how the genetic diversity is generated. In a more detailed analysis of these *de novo* MVs,
401 we classified them as substitutions or SNPs and InDels. We found that the *de novo* MVs
402 generated over sequential passage of both HSV-1 and HSV-2 purified populations were
403 predominately nonconservative changes (Figs 4B and 4C). That was particularly
404 remarkable in the case of HSV-2 populations, where the number of detected
405 nonsynonymous *de novo* SNPs and InDels impacting coding regions gradually and
406 consistently increased, over the ten passages in both cell types and for both purified
407 clones (Figs 4B and 4C, right graphs). These data suggest that the generation of *de novo*
408 genetic diversity in HSV promotes predominantly nonconservative changes.
409 For each *de novo* variant, we also examined its frequency in the population. They were
410 clustered, based on their frequency, in very low frequency MVs (1% to 2%), low
411 frequency MVs (>2% to <10%), medium frequency MVs (10% to <50%), and high
412 frequency variants (equal to or greater than 50%). We observed that the major fraction
413 of *de novo* generated variability corresponded to very low frequency MVs, consistently
414 displayed by almost every purified clone after ten passages in both cell lines (Fig 4D).
415 These very low frequency MVs barely increased in HSV-1 populations after sequential
416 passages, even slightly decreasing as displayed by HSV-1 clone 3, whereas HSV-2
417 clones showed a consistent and significant increment of those. As each HSV-2
418 population was passaged, the very low frequency MVs increased their proportion in the
419 population as the predominant group of MVs. Additionally, we also observed that there

bioRxiv preprint doi: https://doi.org/10.1101/2021.04.09.439146; this version posted April 9, 2021. The copyright holder for this preprint (which was not certified by peer review) is the author/funder, who has granted bioRxiv a license to display the preprint in perpetuity. It is made available under aCC-BY 4.0 International license.

was a gradual and systematic increment of low-medium frequency MVs (taken together) across every viral population of both HSV serotypes (Fig 4D). In this regard, we found that both HSV-2 purified clones remarkably showed the highest increment of low-medium frequency MVs when passaged in HaCaT cells, where HSV-2 clone 5 increased the proportion of these low frequency MVs over the total number of *de novo* variants, from 30% (at P5) to 67% (at P10) (Fig 4D right graph, see S2 Table for details). These data identify these very low frequency MVs as the main source of generation of genetic variability in HSV, gradually increasing as a percentage of the viral population over sequential passage, where each HSV subtype changes with a different speed in response to the same pressures of a given environment.

De novo variants increase the potential coding diversity of HSV-2

After observing that the *de novo* genetic diversity detected after sequential passages in culture was predominantly translated into nonconservative changes for both HSV subtypes, we further examined the distribution of *de novo* MVs impacting coding regions. In accordance with the total number of *de novo* MVs aforementioned (Fig 4A), HSV-1 viral populations displayed an anecdotic low number of MVs impacting just a few genes, while nearly every HSV-2 gene harbored *de novo* MVs (Fig 5). Despite finding an even distribution of *de novo* MVs across the coding genome, some HSV-2 genes were identified as hotspots of novel coding variability (e.g., UL16, UL27, UL28, UL29, UL36). It is also remarkable to observe how the sequential passage of both HSV-2 purified clones in HaCaT cell impacted much more heavily the coding capacity of the HSV-2 genome, as shown in Fig 5, where yellow and orange colors (purified clones passaged in HaCaT cells) dominate over blue tones (passages in Vero cells). Although RL1, RL2, and RS1 genes are located into repetitive areas of the genome, which have been demonstrated to be regions of high variability [38, 40], we also identified a higher number of *de novo* MVs present in these genes after sequential passage of HSV-2 clones in HaCaT cells, compared to Vero cells (Fig 5). As shown in Figs 4B and 4C, for both *de*

bioRxiv preprint doi: https://doi.org/10.1101/2021.04.09.439146; this version posted April 9, 2021. The copyright holder for this preprint (which was not certified by peer review) is the author/funder, who has granted bioRxiv a license to display the preprint in perpetuity. It is made available under aCC-BY 4.0 International license.

448 *novo* appeared SNPs and InDels, intragenic MVs outnumbered those in intergenic
449 regions, despite thinking that higher selective pressures would reduce the appearance
450 of unfavorable mutations in coding regions. These data revealed the impact of very low
451 (1%-2%) and low frequency (<10%) *de novo* MVs in expanding the coding genetic
452 variability in HSV-2, which might have differentially contributed to HSV-2 evolution
453 depending on specific niches.
454
455 **Frequency increase of *de novo* variants may depend on positive selective**
456 **pressure in cell culture**
457 Finally, we examined how the frequency of nonconservative *de novo* variants changed
458 over sequential passages of each purified viral population in both cell types. We found
459 that most of these nonconservative *de novo* MVs did not increase their frequency in the
460 population, seeming to reach a stationary equilibrium or just disappearing after ten
461 passages (S7-S14 Tables). We did not detect any *de novo* InDel in coding regions
462 gradually increasing its frequency in the passaged viral populations, likely reflecting the
463 stronger selective pressure against missense mutations in coding regions. However, a
464 few nonsynonymous *de novo* SNPs were found increasing their frequency significantly
465 in the viral populations, which suggested that those might be conferring a selective
466 advantage. The clearest example for this outcome is illustrated by the syncytia-forming
467 MVs in UL27, as previously described by others [37, 43-45], also observed in the purified
468 HSV-1 clone 3 passaged in Vero cells (Fig 1B). That variant in UL27 (R858H) was not
469 high-confidently detected neither at P0 nor at P5 in Vero cells, *de novo* appearing after
470 P5 and reaching almost a frequency of 50% in the viral population at P10 (Fig 6 left
471 graph, S9 Table). On the other hand, we also observed an interesting positive selection
472 example of a *de novo* variant not conferring a selective advantage in cell culture. We
473 found a nonsynonymous *de novo* variant in the UL13 gene with a frequency of 67%
474 within the HSV-2 clone 1 population after five passages in Vero cells, reaching 90% of
475 the population at P10 (Fig 6 right graph, S11 Table). It has been described that UL13

bioRxiv preprint doi: https://doi.org/10.1101/2021.04.09.439146; this version posted April 9, 2021. The copyright holder for this preprint (which was not certified by peer review) is the author/funder, who has granted bioRxiv a license to display the preprint in perpetuity. It is made available under aCC-BY 4.0 International license.

476 kinase activity is required for axonal transport *in vivo* [47], but it is dispensable *in vitro*
477 [48]. Missense mutations in the UL13 gene have been reported to increase in frequency
478 in different strains of HSV-1 [19, 21, 37, 38]. Thus, it is reasonable to think that the UL13
479 variant found in HSV-2 clone 1 was then not selected based on a selective advantage,
480 but because of the previously observed high tolerance of UL13 inactive kinases. Other
481 MVs, such as those impacting UL14 and UL24 in HSV-2 populations (Fig 6), also
482 reached almost 80-90% of the population at P10. Different variants impacting those
483 genes in HSV-1 have been described, increasing their frequency over sequential
484 passage in cell culture [37], which suggests that nonconservative MVs affecting those
485 genes might confer a selective advantage, or just be more tolerable when HSV replicates
486 *in vitro*.
487
488
489
490
491
492
493
494
495
496
497
498
499
500
501
502
503

bioRxiv preprint doi: https://doi.org/10.1101/2021.04.09.439146; this version posted April 9, 2021. The copyright holder for this preprint (which was not certified by peer review) is the author/funder, who has granted bioRxiv a license to display the preprint in perpetuity. It is made available under aCC-BY 4.0 International license.

DISCUSSION

In this study, we assessed the *de novo* evolution of HSV-1 and HSV-2 generated over sequential passage in two different cell types, using the neurovirulent viral strains SC16 and 333 as a model for each HSV subtype. We characterized for the first time the whole-genome generation of new genetic diversity during viral replication *in vitro*, after having set a high confidence baseline of the preexisting genetic diversity by ultra-deep sequencing of plaque-purified viral populations. This approach allowed us to identify very low frequency *de novo* mutations within genetically homogeneous viral populations, and then examine how viral populations of both HSV serotypes drifted under equal cell culture conditions, in two different cell types. We found that both HSV-1 and HSV-2 increased the number and frequency of *de novo* MVs after five and ten passages, being most of those low frequency nonconservative mutations impacting coding regions. Interestingly, we observed that purified HSV-2 populations were much more prone to generate genetic diversity during passaging than HSV-1, despite displaying a similar number of total preexisting MVs before sequential passages. While the genetic diversity of HSV-1 clonal populations remained similarly stable after being passaged in both Vero and HaCaT cells, HSV-2 purified clones evolved significantly faster when passaged in HaCaT than in Vero cells. HaCaT cells are human skin keratinocytes, an epithelial cell type closer to the natural physiology of HSV infection in the skin. HSV plaque formation, cell-to-cell spread, and cell migration were reported to be significantly different when compared HaCaT to Vero cell infections [46]. In addition, HSV-1 clinical isolates circulating in Finland replicated to lower titers and produced fewer extracellular viral particles in Vero than in HaCaT cells [30]. Since HSV propagation in Vero cells has been the traditional method for viral stock production and *in vitro* studies in virology labs, the evolutionary dynamic shift shown here by HSV-2 in each cell type highlights how critical it is to understand and characterize viral evolution and adaptation in specific cell type cultures. It is instrumental to determine how specific cell-type-associated selective

bioRxiv preprint doi: https://doi.org/10.1101/2021.04.09.439146; this version posted April 9, 2021. The copyright holder for this preprint (which was not certified by peer review) is the author/funder, who has granted bioRxiv a license to display the preprint in perpetuity. It is made available under aCC-BY 4.0 International license.

532 pressures affect our experimental understanding of viral evolution and population
533 dynamics *in vitro*.
534 From these *in vitro* studies, we monitored how genetic drift happened faster in HSV-2
535 than in HSV-1, emphasizing the differential contribution to generate genetic diversity
536 under equal *in vitro* controlled conditions. This lower genetic variability showed by HSV-
537 1 seems to be strain-independent, as recently reported for HSV-1 strain F [37]. Both
538 heterogeneous and purified populations of this HSV-1 strain were sequentially passaged
539 ten times in Vero cells. We quantified the number of *de novo* mutations that appeared
540 over five and ten sequential passages using their available data, finding 19 (P5) and 7
541 (P10) *de novo* MVs (≥2%) not listed at P0 for the heterogeneous population (Mixed as
542 referred in the original article), while 3 (P5) and 4 (P10) *de novo* MVs were detected in
543 the purified population. These numbers are similar to the number of *de novo* mutations
544 (≥2%) that we found for HSV-1 strain SC16 purified populations in both cell types. Before
545 the high-throughput sequencing era, it was also reported that the spontaneous mutation
546 rate in laboratory strains of HSV-2 (including the 333 strain) was 9- to 16-fold more
547 frequent than that in HSV-1 SC16, when selecting drug-resistant mutants in cell culture
548 [25]. These data correlate with our findings observed from the genome-wide analysis of
549 genetic diversity, where HSV-2 populations generated a 5-fold higher number of variants
550 than HSV-1 counterparts in Vero cells, but 10-fold higher when passaged in HaCaT cells.
551 On the other hand, different studies describing the genetic diversity found in clinical
552 isolates of both serotypes, by high-throughput sequencing technologies, also support
553 that HSV-2 is more prone to generate nonconservative genetic diversity than HSV-1 also
554 *in vivo*. Seven uncultured swab specimens of genital HSV-1 showed a total of 114
555 summed variants (≥2%) [34], while 10 HSV-1 clinical isolates from Finland exhibited less
556 than 150 grouped variants, mainly localized at repeated regions [30]. However, when ten
557 neonatal HSV-2 isolates were examined, a total of 1,821 variants was found, of which
558 784 were found across 71 genes [31]. The degree of coding diversity was also similar

bioRxiv preprint doi: https://doi.org/10.1101/2021.04.09.439146; this version posted April 9, 2021. The copyright holder for this preprint (which was not certified by peer review) is the author/funder, who has granted bioRxiv a license to display the preprint in perpetuity. It is made available under aCC-BY 4.0 International license.

559 when compared to a different set of 10 adult HSV-2 isolates. Additionally, it was also
560 reported that HSV-2 isolates generated drug-resistant mutants 30 times faster than HSV-
561 1 clinical isolates [25]. It seems reasonable to attribute the higher mutation frequency of
562 HSV-2 to a lower fidelity of its polymerase during viral replication. Nevertheless, HSV-1
563 recombinants expressing HSV-2 polymerase were reported to have similar error rates to
564 HSV-1 parental homologs, suggesting that the polymerase would not be solely
565 responsible for these serotype-specific differences in mutation frequency, and other viral
566 proteins and secondary structures of the genome might contribute to explain it [49].
567 These experiments emphasized the critical value and usefulness of using *de novo*
568 assembled consensus genomes generated from the actual stocks under study [41, 42],
569 as well as of using purified homogeneous viral populations from the exact parental
570 stocks. These previously described consensus genomes for strains SC16 and 333
571 represented with higher accuracy the structural and genetic heterogenicity contained into
572 each parental stock, rather than having used reference strain genomes commonly used
573 for comparative genomics [35]. The reduction of the initial genetic variability contained
574 into each original viral stock by plaque-picked isolation of subclones, contributed to set
575 a more uniform baseline to identify new generated MVs during viral replication. Some
576 genome-wide studies of HSV-1 revealed approximately 3-4% of nucleotide variation
577 genome-wide, being reduced up to 1-2% after plaque-purification of subclones [21, 40,
578 50]. We reduced this genome-wide nucleotide variation rate from 0.47% (712 MVs /
579 150,000 bp) and 0.7% (1044 MVs) to an average of 0.08% (118 MVs) and 0.1% (145
580 MVs), between five times plaque-purified clones and their parental stocks for HSV-1 and
581 HSV-2, respectively. Nonetheless, it has been reported that the extreme genetic
582 bottleneck induced by this isolation technique can cause severe attenuation of mortality
583 in mice, even the complete loss of *in vitro* replicative capacity [39]. Characterizing the
584 biological phenotype of these plaque-isolated subclones is essential to ensure that the
585 genetic bottleneck exerted by the experimental approach has not altered the virus
586 biology. The measurement of these phenotypes may include classical measures, such

bioRxiv preprint doi: https://doi.org/10.1101/2021.04.09.439146; this version posted April 9, 2021. The copyright holder for this preprint (which was not certified by peer review) is the author/funder, who has granted bioRxiv a license to display the preprint in perpetuity. It is made available under aCC-BY 4.0 International license.

as plaque morphology or replication kinetics, and *in vivo* measures of pathogenesis. This connection between comparative genomic studies to the measurement of biological phenotypes is critical to integrate previous phenotypic effects of over-expression, deletion, and modifications of defined loci with the new insights from comparative genomic studies.

From a technical perspective, this study highlights the importance of ultra-deep sequencing for the identification of *de novo* genetic diversity, since greater coverage depth is directly translated into higher confidence when identifying MVs. Only a few complete rounds of viral replication occur in a single passage in cell culture, where *de novo* MVs would be represented with a very low frequency within the replicating population. If these new variants are not beneficial or are just tolerable in terms of viral fitness, they might not increase their frequency enough in the population to be detectable by standard-deep sequencing, which average coverage ranges between 100-1000X [30, 31, 33, 34, 37]. Those and other studies generally reported only MVs above 2%, accepted as the minimum frequency threshold cut-off. If so, with a 100X coverage, a 2% threshold for MVs calling would mean that only two sequencing reads were required to detect the minor variant. In order to be able to lower this threshold to 1%, we increased the coverage cut-off greater than 200X. On top of these, we implemented an additional filter to allow the call of those MVs with high frequency but below the 200X coverage threshold, proportionally increasing the coverage needed for positive filtering as lower the frequency was. These comprehensive quality controls, together with the benefits provided by an ultra-deep sequence coverage, are instrumental in detecting very low MVs and minimizing the chance of calling false positives. The integration of comparative genomic and reverse genetic approaches will improve our understanding of fundamental aspects of HSV biology, where studying the phenotypic effect of *in vitro* and *in vivo* generated variants can complement previous discoveries on gene roles, as well as explaining or predicting clinical outcomes.

bioRxiv preprint doi: https://doi.org/10.1101/2021.04.09.439146; this version posted April 9, 2021. The copyright holder for this preprint (which was not certified by peer review) is the author/funder, who has granted bioRxiv a license to display the preprint in perpetuity. It is made available under aCC-BY 4.0 International license.

The human herpesviruses literature shows how researchers have used cell lines, commonly Vero cells, to generate high titer stocks of both laboratory-adapted strains but also to amplify scarce clinical samples to decipher the *in vitro* and *in vivo* aspects of HSV biology. Most of the HSV comparative genomic studies have also used *in vitro* amplification to generate a high yield of viral genomic DNA for the preparation of high-quality sequencing libraries. Other authors pointed out that growing HSV in cell culture is clearly different from how the virus would replicate within its human host, where selective pressures and genetic bottlenecks must be substantially different between these two replicative scenarios [37, 40, 51]. However, here for the first time, we have identified and characterized how the genetic diversity is differentially generated between human herpesviruses when serially passaged in cell culture. The effects that this differentially generated genetic diversity may have had on each aspect of HSV biology, as well as on the clinical outcomes of infections, is currently an active area of research [52].

Alphaherpesviruses are no longer seen as a static and homogeneous population but as such presenting *in vivo* heterogeneous diversity [34, 53]. HSV-1 and HSV-2 exhibit a remarkably unequal global seroprevalence and preference for infecting different anatomical areas, where each cellular environment may have exerted differential selective pressures over viral replication, latency and reactivation. These unique selective pressures, found at each epithelial and neuronal tissue of the oronasal and genital areas, might have contributed to their evolutionary divergence and differential genetic drift rate. A better understanding of how human herpesviruses mutate during each phase of their life cycle will provide a better knowledge on sequence determinants of virulence factors and will help to monitor resistance to anti-viral drugs.

bioRxiv preprint doi: https://doi.org/10.1101/2021.04.09.439146; this version posted April 9, 2021. The copyright holder for this preprint (which was not certified by peer review) is the author/funder, who has granted bioRxiv a license to display the preprint in perpetuity. It is made available under aCC-BY 4.0 International license.

MATERIALS AND METHODS

Cells and viruses

Vero (*Cercopithecus aethiops* kidney epithelial) cells (ATCC, CCL-81) and HaCaT (human epithelial keratinocytes) cells (Section of Virology, Department of Infectious Disease, Imperial College London [54]) were maintained at 37ºC with 5 percent CO_2. Cells were cultured in Dulbecco's Modified Eagle's Medium (DMEM) supplemented with 5% (v/v) Fetal Bovine Serum (FBS), 2 mM L-glutamine, and antibiotics (75 µg/ml penicillin, 75 U/ml streptomycin, and 25 µg/ml gentamycin). Cells were regularly tested for mycoplasma contaminations by standard PCR with primers Myco_Fw (GGCGAATGGCTGAGTAACACG) and Myco_Rv (CGGATAACGCTTGCGACCTAT). HSV-1 strain SC16 and HSV-2 strain 333 original stocks were kindly provided by Dr. Helena Browne, University of Cambridge (UK). The genome sequence of plaque purified viral clones from original stocks are GenBank available under accession no. KX946970 for HSV-1 strain SC16 [42], and under accession no. LS480640 for HSV-2 strain 333 [41].

High-throughput sequencing

High-throughput sequencing was performed in a similar manner as previously described [41, 42]. Briefly, viral DNA was prepared by infection of one confluent P150-cm^2 plate of Vero cells (MOI = 5 PFU/cell). Cells and supernatant were collected when reaching 90-100% of cytopathic effect. Viral nucleocapsids were extracted by mechanical disruption of the cellular pellet and clarified by cellular debris after 10 min of centrifugation at 300 x *g*. Viral particles were treated with DNAse I, RNAse A, and nuclease S7 to eliminate remaining cellular DNA/RNA, and nuclease activity was then inactivated with EDTA-EGTA. Nucleocapsids were then lysed using sodium dodecyl sulfate and Proteinase K, and viral genomic DNA was purified using phenol-chloroform-isoamyl alcohol. Potential contaminating DNA was checked by PCR against mycoplasma, prokaryotic 16S rRNA

bioRxiv preprint doi: https://doi.org/10.1101/2021.04.09.439146; this version posted April 9, 2021. The copyright holder for this preprint (which was not certified by peer review) is the author/funder, who has granted bioRxiv a license to display the preprint in perpetuity. It is made available under aCC-BY 4.0 International license.

(primers 16S_Fw: CCTACGGGNBGCASCAG, and 16S_Rv: GACTACNVGGGTATCTAATCC) and eukaryotic 18S rRNA (primers 18S_Fw: GCCAGCAVCYGCGGTAAY, and 18S_Rv: CCGTCAATTHCTTYAART) [55, 56]. Finally, viral DNA was tested by PCR to determine HSV-type cross-contamination (primers Up_US4(1)_Fw: AGCGCCGTTGACTACATTCAC, and Dw_US4(1)_Rv: GCGCACCGGTGATTTATACCA, for HSV-1; Up_US4(2)_Fw: TCTTGAGCGCCATCGACTACG, and Dw_US4(2)_Rv: CCGCTCCATAGCTGCTGTACC, for HSV-2). An aliquot of viral genomic DNA (100 ng) was submitted to MicrobesNG, University of Birmingham (UK), to prepare barcode sequencing libraries, according to the NEBNext Ultra DNA Library Prep kit instructions (New England Biolabs). Libraries were quantified by Qubit (Invitrogen, CA), assessed by Bioanalyzer (Agilent), and library adapter qPCR (KAPA Biosystems). Sequencing was performed on an Illumina MiSeq device as paired-end reads (2 x 250 bp), according to the manufacturer's recommendations. Sequencing statistics for every sample used in this study can be found in S1 Table.

Selection of viral clones from original stocks

Five plaque-purified viral clones from both HSV-1 (SC16) and HSV-2 (333) original stocks were isolated by plaque isolation. Vero cell monolayers with 5 x 10^5 cells/well in 6-well plates were infected at an MOI of 0.01 PFU/cell. After 48 hours post-infection (hpi), defined and single viral plaques were carefully isolated by fine pipetting 10 µl of media containing the selected plaque. Then, 30 µl of fresh media were added to each isolated plaque, followed by three rounds of freezing and thawing. An aliquot of 1 µl was three times serially diluted to infect fresh Vero cells monolayer in 6-well plates. After five subsequent rounds, one confluent P150-cm^2 plate of Vero cells was infected in order to produce a viral stock for sequencing and subsequent infections.

***In vitro* generation of genetic variability experiments**

bioRxiv preprint doi: https://doi.org/10.1101/2021.04.09.439146; this version posted April 9, 2021. The copyright holder for this preprint (which was not certified by peer review) is the author/funder, who has granted bioRxiv a license to display the preprint in perpetuity. It is made available under aCC-BY 4.0 International license.

Two selected plaque-purified clones from HSV-1 and HSV-2 original stocks were used to infect a P60-cm^2 plate of Vero and HaCaT cells separately at an MOI of 0.1 PFU/cell. After 2 hpi, the viral inoculum was removed and fresh DMEM with 2% FBS was added. Forty-eight hpi viruses were harvested by collecting both cells and supernatant, followed by three freezing and thawing cycles. Each cycle of infection and harvest was considered a passage. The harvested viruses were then used to infect the next fresh plate of Vero or HaCaT cells (estimated MOI of 0.1 PFU/cell). Each selected clone was passaged ten times in each cell line. Passages from 4th to 5th and 9th to 10th were made by infecting one confluent P150-cm^2 plate of corresponding cells (adjusting the MOI), in order to obtain higher yields of viral DNA for sequencing.

Genetic variant analysis and identification of *de novo* variants

Reads from each sequenced sample were trimmed using Trimmomatic v0.36 [57], quality-filtered with PrinSeq v1.2 [58], and aligned against the reference sequence for each case, by using Bowtie 2 v2.3.4.1 [59], with default settings. Alignments were visualized using Integrative Genomics Viewer v2.8.2 [60] to detect large gaps and rearrangements. MVs present in each sequenced viral population were detected by using VarScan v2.4.3 [61], with settings intended to minimize sequencing-induced errors from the raw calling of MVs: minimum variant allele frequency ≥0.01 (1%); minimum coverage ≥20, base call quality ≥20, exclusion of variants supported on one strand by >90 percent. Detected MVs from VarScan calling were then annotated onto their corresponding genome to determine their mutational effects. MVs were then additionally filtered by coverage >200. An additional filter was implemented in order to detect those MVs with high frequency but low coverage, where read depth at the given position had to be greater than the product obtained from dividing 200 (coverage threshold) by the variant frequency (0-100) at the given position:

$$read\ depth\ at\ the\ given\ position > \left(\frac{200\ (Coverage\ threshold)}{frequency\ (0-100)}\right)$$

bioRxiv preprint doi: https://doi.org/10.1101/2021.04.09.439146; this version posted April 9, 2021. The copyright holder for this preprint (which was not certified by peer review) is the author/funder, who has granted bioRxiv a license to display the preprint in perpetuity. It is made available under aCC-BY 4.0 International license.

MVs were considered as *de novo* appearance when, after coverage filtering, its frequency in the previous parental viral population was inexistent or < 0.01. Coverage plots for each alignment, as well as detected MVs in each viral population, were represented across their corresponding genome, according to their location and frequency (S1-S3 and S5-S9 Figs). For a summary list of detected, filtered, and categorized MVs for every sample sequenced in this study, see S2 Table. For a full list of MVs detected in each viral population, see S3 Table (HSV-1 original stock and isolated clones), S4 Table (HSV-2 original stock and isolated clones), S5 Table (ultra-deep sequencing of HSV-1 clones 2 and 3), S6 Table (ultra-deep sequencing of HSV-2 clones 2 and 3), S7 and S8 Tables (HSV-1 clone 2 in Vero and HaCaT cells, respectively), S9 and S10 Tables (HSV-1 clone 3 in Vero and HaCaT cells, respectively), S11 and S12 Tables (HSV-2 clone 1 in Vero and HaCaT cells, respectively), and S13 and S14 Tables (HSV-2 clone 5 in Vero and HaCaT cells, respectively).

Statistical analysis

All statistical analyses were performed using GraphPad Prism 8 (v8.4.3) software. Two-tailed Mann–Whitney *U*-test was used with the number of MVs analyses ($p < 0.05$).

Data availability

Consensus genomes of a plaque purified viral clone from each original stock were retrieved from GenBank as follows: KX946970 for HSV-1 strain SC16; LS480640 for HSV-2 strain 333. Raw sequence reads are available at the European Bioinformatics Institute (EMBL-EBI) European Nucleotide Archive (ENA) as Bioproject ID PRJEB32133 and PRJEB32148.

bioRxiv preprint doi: https://doi.org/10.1101/2021.04.09.439146; this version posted April 9, 2021. The copyright holder for this preprint (which was not certified by peer review) is the author/funder, who has granted bioRxiv a license to display the preprint in perpetuity. It is made available under aCC-BY 4.0 International license.

ACKNOWLEDGMENTS

We thank Anthony Minson and Helena Brown (University of Cambridge, UK) for kindly providing the HSV-1 strain SC16 and HSV-2 strain 333 viral stocks, respectively. We are grateful to the Genomics and Next Generation Sequencing Service at Centro de Biología Molecular Severo Ochoa for their support and advice. Genome sequencing was provided by MicrobesNG (http://www.microbesng.uk), which is supported by the BBSRC (grant no. BB/L024209/1).

bioRxiv preprint doi: https://doi.org/10.1101/2021.04.09.439146; this version posted April 9, 2021. The copyright holder for this preprint (which was not certified by peer review) is the author/funder, who has granted bioRxiv a license to display the preprint in perpetuity. It is made available under aCC-BY 4.0 International license.

781 **REFERENCES**

782

783 1. James C, Harfouche M, Welton NJ, Turner KM, Abu-Raddad LJ, Gottlieb SL, et
784 al. Herpes simplex virus: global infection prevalence and incidence estimates, 2016. Bull
785 World Health Organ. 2020;98(5):315-29. doi: 10.2471/BLT.19.237149. PubMed PMID:
786 32514197.
787 2. Forward KR, Lee SH. Predominance of herpes simplex virus type 1 from patients
788 with genital herpes in Nova Scotia. Can J Infect Dis. 2003;14(2):94-6. doi:
789 10.1155/2003/168673. PubMed PMID: 18159431.
790 3. Wald A, Ericsson M, Krantz E, Selke S, Corey L. Oral shedding of herpes simplex
791 virus type 2. Sex Transm Infect. 2004;80(4):272-6. doi: 10.1136/sti.2003.007823.
792 PubMed PMID: 15295123.
793 4. Gupta R, Warren T, Wald A. Genital herpes. Lancet. 2007;370(9605):2127-37.
794 Epub 2007/12/25. doi: 10.1016/S0140-6736(07)61908-4. PubMed PMID: 18156035.
795 5. Ayoub HH, Chemaitelly H, Abu-Raddad LJ. Characterizing the transitioning
796 epidemiology of herpes simplex virus type 1 in the USA: model-based predictions. BMC
797 Med. 2019;17(1):57. doi: 10.1186/s12916-019-1285-x. PubMed PMID: 30853029.
798 6. Knipe DM, Cliffe A. Chromatin control of herpes simplex virus lytic and latent
799 infection. Nat Rev Microbiol. 2008;6(3):211-21. doi: 10.1038/nrmicro1794. PubMed
800 PMID: 18264117.
801 7. Kawaguchi Y, Mori Y, Kimura H. Human Herpesviruses: Springer; 2018.
802 8. Roizman B, D.M. Knipe, and R. Whitley. Herpes Simplex Viruses. Fields
803 Virology. 6th ed. Philadelphia, PA: Lippincott Williams and Wilkins; 2013. p. 1823-97.
804 9. Kennedy PG, Rovnak J, Badani H, Cohrs RJ. A comparison of herpes simplex
805 virus type 1 and varicella-zoster virus latency and reactivation. J Gen Virol. 2015;96(Pt
806 7):1581-602. doi: 10.1099/vir.0.000128. PubMed PMID: 25794504.
807 10. Lieberman PM. Epigenetics and Genetics of Viral Latency. Cell Host Microbe.
808 2016;19(5):619-28. doi: 10.1016/j.chom.2016.04.008. PubMed PMID: 27173930.

bioRxiv preprint doi: https://doi.org/10.1101/2021.04.09.439146; this version posted April 9, 2021. The copyright holder for this preprint (which was not certified by peer review) is the author/funder, who has granted bioRxiv a license to display the preprint in perpetuity. It is made available under aCC-BY 4.0 International license.

809 11. Drake JW, Hwang CB. On the mutation rate of herpes simplex virus type 1.
810 Genetics. 2005;170(2):969-70. doi: 10.1534/genetics.104.040410. PubMed PMID:
811 15802515.
812 12. Sanjuán R, Nebot MR, Chirico N, Mansky LM, Belshaw R. Viral mutation rates. J
813 Virol. 2010;84(19):9733-48. doi: 10.1128/JVI.00694-10. PubMed PMID: 20660197.
814 13. McCrone JT, Lauring AS. Genetic bottlenecks in intraspecies virus transmission.
815 Curr Opin Virol. 2018;28:20-5. doi: 10.1016/j.coviro.2017.10.008. PubMed PMID:
816 29107838.
817 14. Mahiet C, Ergani A, Huot N, Alende N, Azough A, Salvaire F, et al. Structural
818 variability of the herpes simplex virus 1 genome in vitro and in vivo. J Virol.
819 2012;86(16):8592-601. doi: 10.1128/JVI.00223-12. PubMed PMID: 22674981.
820 15. Chou J, Roizman B. Isomerization of herpes simplex virus 1 genome:
821 identification of the cis-acting and recombination sites within the domain of the a
822 sequence. Cell. 1985;41(3):803-11. doi: 10.1016/s0092-8674(85)80061-1. PubMed
823 PMID: 2988789.
824 16. Huang KJ, Zemelman BV, Lehman IR. Endonuclease G, a candidate human
825 enzyme for the initiation of genomic inversion in herpes simplex type 1 virus. J Biol
826 Chem. 2002;277(23):21071-9. doi: 10.1074/jbc.M201785200. PubMed PMID:
827 11912214.
828 17. Muylaert I, Tang KW, Elias P. Replication and recombination of herpes simplex
829 virus DNA. J Biol Chem. 2011;286(18):15619-24. doi: 10.1074/jbc.R111.233981.
830 PubMed PMID: 21362621.
831 18. Norberg P, Kasubi MJ, Haarr L, Bergstrom T, Liljeqvist JA. Divergence and
832 recombination of clinical herpes simplex virus type 2 isolates. J Virol.
833 2007;81(23):13158-67. doi: 10.1128/jvi.01310-07. PubMed PMID: 17881457.
834 19. Lee K, Kolb AW, Sverchkov Y, Cuellar JA, Craven M, Brandt CR. Recombination
835 Analysis of Herpes Simplex Virus 1 Reveals a Bias toward GC Content and the Inverted

bioRxiv preprint doi: https://doi.org/10.1101/2021.04.09.439146; this version posted April 9, 2021. The copyright holder for this preprint (which was not certified by peer review) is the author/funder, who has granted bioRxiv a license to display the preprint in perpetuity. It is made available under aCC-BY 4.0 International license.

836 Repeat Regions. J Virol. 2015;89(14):7214-23. doi: 10.1128/JVI.00880-15. PubMed
837 PMID: 25926637.
838 20. Koelle DM, Norberg P, Fitzgibbon MP, Russell RM, Greninger AL, Huang ML, et
839 al. Worldwide circulation of HSV-2 x HSV-1 recombinant strains. Sci Rep. 2017;7:44084.
840 doi: 10.1038/srep44084. PubMed PMID: 28287142.
841 21. Szpara ML, Gatherer D, Ochoa A, Greenbaum B, Dolan A, Bowden RJ, et al.
842 Evolution and diversity in human herpes simplex virus genomes. J Virol.
843 2014;88(2):1209-27. doi: 10.1128/JVI.01987-13. PubMed PMID: 24227835.
844 22. Hall JD, Almy RE. Evidence for control of herpes simplex virus mutagenesis by
845 the viral DNA polymerase. Virology. 1982;116(2):535-43. doi: 10.1016/0042-
846 6822(82)90146-5. PubMed PMID: 6278726.
847 23. Brown J. Effect of gene location on the evolutionary rate of amino acid
848 substitutions in herpes simplex virus proteins. Virology. 2004;330(1):209-20. doi:
849 10.1016/j.virol.2004.09.020. PubMed PMID: 15527847.
850 24. Parris DS, Harrington JE. Herpes simplex virus variants restraint to high
851 concentrations of acyclovir exist in clinical isolates. Antimicrob Agents Chemother.
852 1982;22(1):71-7. doi: 10.1128/aac.22.1.71. PubMed PMID: 6289742.
853 25. Sarisky RT, Nguyen TT, Duffy KE, Wittrock RJ, Leary JJ. Difference in incidence
854 of spontaneous mutations between herpes simplex virus types 1 and 2. Antimicrob
855 Agents Chemother. 2000;44(6):1524-9. doi: 10.1128/aac.44.6.1524-1529.2000.
856 PubMed PMID: 10817703.
857 26. Burrel S, Deback C, Agut H, Boutolleau D. Genotypic characterization of UL23
858 thymidine kinase and UL30 DNA polymerase of clinical isolates of herpes simplex virus:
859 natural polymorphism and mutations associated with resistance to antivirals. Antimicrob
860 Agents Chemother. 2010;54(11):4833-42. doi: 10.1128/AAC.00669-10. PubMed PMID:
861 20733037.

bioRxiv preprint doi: https://doi.org/10.1101/2021.04.09.439146; this version posted April 9, 2021. The copyright holder for this preprint (which was not certified by peer review) is the author/funder, who has granted bioRxiv a license to display the preprint in perpetuity. It is made available under aCC-BY 4.0 International license.

862 27. Sauerbrei A, Deinhardt S, Zell R, Wutzler P. Phenotypic and genotypic
863 characterization of acyclovir-resistant clinical isolates of herpes simplex virus. Antiviral
864 Res. 2010;86(3):246-52. doi: 10.1016/j.antiviral.2010.03.002. PubMed PMID: 20211650.
865 28. Renzette N, Bhattacharjee B, Jensen JD, Gibson L, Kowalik TF. Extensive
866 genome-wide variability of human cytomegalovirus in congenitally infected infants. PLoS
867 Pathog. 2011;7(5):e1001344. doi: 10.1371/journal.ppat.1001344. PubMed PMID:
868 21625576.
869 29. Sanjuán R, Domingo-Calap P. Mechanisms of viral mutation. Cell Mol Life Sci.
870 2016;73(23):4433-48. doi: 10.1007/s00018-016-2299-6. PubMed PMID: 27392606.
871 30. Bowen CD, Paavilainen H, Renner DW, Palomaki J, Lehtinen J, Vuorinen T, et
872 al. Comparison of Herpes Simplex Virus 1 Strains Circulating in Finland Demonstrates
873 the Uncoupling of Whole-Genome Relatedness and Phenotypic Outcomes of Viral
874 Infection. J Virol. 2019;93(8). doi: 10.1128/JVI.01824-18. PubMed PMID: 30760568.
875 31. Akhtar LN, Bowen CD, Renner DW, Pandey U, Della Fera AN, Kimberlin DW, et
876 al. Genotypic and Phenotypic Diversity of Herpes Simplex Virus 2 within the Infected
877 Neonatal Population. mSphere. 2019;4(1). doi: 10.1128/mSphere.00590-18. PubMed
878 PMID: 30814317.
879 32. Depledge DP, Gray ER, Kundu S, Cooray S, Poulsen A, Aaby P, et al. Evolution
880 of cocirculating varicella-zoster virus genotypes during a chickenpox outbreak in Guinea-
881 Bissau. J Virol. 2014;88(24):13936-46. doi: 10.1128/JVI.02337-14. PubMed PMID:
882 25275123.
883 33. Hage E, Wilkie GS, Linnenweber-Held S, Dhingra A, Suarez NM, Schmidt JJ, et
884 al. Characterization of Human Cytomegalovirus Genome Diversity in
885 Immunocompromised Hosts by Whole-Genome Sequencing Directly From Clinical
886 Specimens. J Infect Dis. 2017;215(11):1673-83. doi: 10.1093/infdis/jix157. PubMed
887 PMID: 28368496.
888 34. Shipley MM, Renner DW, Ott M, Bloom DC, Koelle DM, Johnston C, et al.
889 Genome-Wide Surveillance of Genital Herpes Simplex Virus Type 1 From Multiple

bioRxiv preprint doi: https://doi.org/10.1101/2021.04.09.439146; this version posted April 9, 2021. The copyright holder for this preprint (which was not certified by peer review) is the author/funder, who has granted bioRxiv a license to display the preprint in perpetuity. It is made available under aCC-BY 4.0 International license.

890 Anatomic Sites Over Time. J Infect Dis. 2018;218(4):595-605. doi: 10.1093/infdis/jiy216.
891 PubMed PMID: 29920588.
892 35. Renner DW, Szpara ML. Impacts of Genome-Wide Analyses on Our
893 Understanding of Human Herpesvirus Diversity and Evolution. J Virol. 2018;92(1). doi:
894 10.1128/jvi.00908-17. PubMed PMID: 29046445.
895 36. Mosca JD, Pitha PM. Transcriptional and posttranscriptional regulation of
896 exogenous human beta interferon gene in simian cells defective in interferon synthesis.
897 Mol Cell Biol. 1986;6(6):2279-83. doi: 10.1128/mcb.6.6.2279. PubMed PMID: 3785197.
898 37. Kuny CV, Bowen CD, Renner DW, Johnston CM, Szpara ML. In vitro evolution
899 of herpes simplex virus 1 (HSV-1) reveals selection for syncytia and other minor variants
900 in cell culture. Virus Evol. 2020;6(1):veaa013. doi: 10.1093/ve/veaa013. PubMed PMID:
901 32296542.
902 38. Szpara ML, Parsons L, Enquist LW. Sequence variability in clinical and laboratory
903 isolates of herpes simplex virus 1 reveals new mutations. J Virol. 2010;84(10):5303-13.
904 doi: 10.1128/jvi.00312-10. PubMed PMID: 20219902.
905 39. Jaramillo N, Domingo E, Munoz-Egea MC, Tabares E, Gadea I. Evidence of
906 Muller's ratchet in herpes simplex virus type 1. J Gen Virol. 2013;94(Pt 2):366-75. doi:
907 10.1099/vir.0.044685-0. PubMed PMID: 23100362.
908 40. Parsons LR, Tafuri YR, Shreve JT, Bowen CD, Shipley MM, Enquist LW, et al.
909 Rapid genome assembly and comparison decode intrastrain variation in human
910 alphaherpesviruses. MBio. 2015;6(2). doi: 10.1128/mBio.02213-14. PubMed PMID:
911 25827418.
912 41. Lopez-Munoz AD, Rastrojo A, Alcami A. Complete Genome Sequence of Herpes
913 Simplex Virus 2 Strain 333. Microbiol Resour Announc. 2018;7(9). doi:
914 10.1128/MRA.00870-18. PubMed PMID: 30533931.
915 42. Rastrojo A, Lopez-Munoz AD, Alcami A. Genome Sequence of Herpes Simplex
916 Virus 1 Strain SC16. Genome Announc. 2017;5(4). doi: 10.1128/genomeA.01392-16.
917 PubMed PMID: 28126930.

bioRxiv preprint doi: https://doi.org/10.1101/2021.04.09.439146; this version posted April 9, 2021. The copyright holder for this preprint (which was not certified by peer review) is the author/funder, who has granted bioRxiv a license to display the preprint in perpetuity. It is made available under aCC-BY 4.0 International license.

43. Bzik DJ, Fox BA, DeLuca NA, Person S. Nucleotide sequence of a region of the herpes simplex virus type 1 gB glycoprotein gene: mutations affecting rate of virus entry and cell fusion. Virology. 1984;137(1):185-90. doi: 10.1016/0042-6822(84)90022-9. PubMed PMID: 6089415.

44. Engel JP, Boyer EP, Goodman JL. Two novel single amino acid syncytial mutations in the carboxy terminus of glycoprotein B of herpes simplex virus type 1 confer a unique pathogenic phenotype. Virology. 1993;192(1):112-20. doi: 10.1006/viro.1993.1013. PubMed PMID: 8390747.

45. Diakidi-Kosta A, Michailidou G, Kontogounis G, Sivropoulou A, Arsenakis M. A single amino acid substitution in the cytoplasmic tail of the glycoprotein B of herpes simplex virus 1 affects both syncytium formation and binding to intracellular heparan sulfate. Virus Res. 2003;93(1):99-108. doi: 10.1016/s0168-1702(03)00070-4. PubMed PMID: 12727347.

46. Abaitua F, Zia FR, Hollinshead M, O'Hare P. Polarized cell migration during cell-to-cell transmission of herpes simplex virus in human skin keratinocytes. J Virol. 2013;87(14):7921-32. doi: 10.1128/jvi.01172-13. PubMed PMID: 23658449.

47. Coller KE, Smith GA. Two viral kinases are required for sustained long distance axon transport of a neuroinvasive herpesvirus. Traffic. 2008;9(9):1458-70. doi: 10.1111/j.1600-0854.2008.00782.x. PubMed PMID: 18564370.

48. Gershburg S, Geltz J, Peterson KE, Halford WP, Gershburg E. The UL13 and US3 Protein Kinases of Herpes Simplex Virus 1 Cooperate to Promote the Assembly and Release of Mature, Infectious Virions. PLoS One. 2015;10(6):e0131420. doi: 10.1371/journal.pone.0131420. PubMed PMID: 26115119.

49. Duffy KE, Quail MR, Nguyen TT, Wittrock RJ, Bartus JO, Halsey WM, et al. Assessing the contribution of the herpes simplex virus DNA polymerase to spontaneous mutations. BMC Infect Dis. 2002;2:7. doi: 10.1186/1471-2334-2-7. PubMed PMID: 12019036.

bioRxiv preprint doi: https://doi.org/10.1101/2021.04.09.439146; this version posted April 9, 2021. The copyright holder for this preprint (which was not certified by peer review) is the author/funder, who has granted bioRxiv a license to display the preprint in perpetuity. It is made available under aCC-BY 4.0 International license.

945 50. Bowen CD, Renner DW, Shreve JT, Tafuri Y, Payne KM, Dix RD, et al. Viral
946 forensic genomics reveals the relatedness of classic herpes simplex virus strains KOS,
947 KOS63, and KOS79. Virology. 2016;492:179-86. doi: 10.1016/j.virol.2016.02.013.
948 PubMed PMID: 26950505.
949 51. Wilkinson GW, Davison AJ, Tomasec P, Fielding CA, Aicheler R, Murrell I, et al.
950 Human cytomegalovirus: taking the strain. Medical microbiology and immunology.
951 2015;204(3):273-84. doi: 10.1007/s00430-015-0411-4. PubMed PMID: 25894764.
952 52. Kuny CV, Szpara ML. Alphaherpesvirus Genomics: Past, Present and Future.
953 Curr Issues Mol Biol. 2020;42:41-80. doi: 10.21775/cimb.042.041. PubMed PMID:
954 33159012.
955 53. Minaya MA, Jensen TL, Goll JB, Korom M, Datla SH, Belshe RB, et al. Molecular
956 Evolution of Herpes Simplex Virus 2 Complete Genomes: Comparison between Primary
957 and Recurrent Infections. J Virol. 2017;91(23). doi: 10.1128/jvi.00942-17. PubMed
958 PMID: 28931680.
959 54. Boukamp P, Petrussevska RT, Breitkreutz D, Hornung J, Markham A, Fusenig
960 NE. Normal keratinization in a spontaneously immortalized aneuploid human
961 keratinocyte cell line. J Cell Biol. 1988;106(3):761-71. PubMed PMID: 2450098.
962 55. Hugerth LW, Muller EE, Hu YO, Lebrun LA, Roume H, Lundin D, et al. Systematic
963 design of 18S rRNA gene primers for determining eukaryotic diversity in microbial
964 consortia. PLoS One. 2014;9(4):e95567. doi: 10.1371/journal.pone.0095567. PubMed
965 PMID: 24755918.
966 56. Takahashi S, Tomita J, Nishioka K, Hisada T, Nishijima M. Development of a
967 prokaryotic universal primer for simultaneous analysis of Bacteria and Archaea using
968 next-generation sequencing. PLoS One. 2014;9(8):e105592. doi:
969 10.1371/journal.pone.0105592. PubMed PMID: 25144201.
970 57. Bolger AM, Lohse M, Usadel B. Trimmomatic: a flexible trimmer for Illumina
971 sequence data. Bioinformatics. 2014;30(15):2114-20. doi:
972 10.1093/bioinformatics/btu170. PubMed PMID: 24695404.

bioRxiv preprint doi: https://doi.org/10.1101/2021.04.09.439146; this version posted April 9, 2021. The copyright holder for this preprint (which was not certified by peer review) is the author/funder, who has granted bioRxiv a license to display the preprint in perpetuity. It is made available under aCC-BY 4.0 International license.

973 58. Schmieder R, Edwards R. Quality control and preprocessing of metagenomic
974 datasets. Bioinformatics. 2011;27(6):863-4. doi: 10.1093/bioinformatics/btr026. PubMed
975 PMID: 21278185.
976 59. Langmead B, Salzberg SL. Fast gapped-read alignment with Bowtie 2. Nat
977 Methods. 2012;9(4):357-9. doi: 10.1038/nmeth.1923. PubMed PMID: 22388286.
978 60. Robinson JT, Thorvaldsdóttir H, Winckler W, Guttman M, Lander ES, Getz G, et
979 al. Integrative genomics viewer. Nat Biotechnol. 2011;29(1):24-6. doi: 10.1038/nbt.1754.
980 PubMed PMID: 21221095.
981 61. Koboldt DC, Zhang Q, Larson DE, Shen D, McLellan MD, Lin L, et al. VarScan
982 2: somatic mutation and copy number alteration discovery in cancer by exome
983 sequencing. Genome Res. 2012;22(3):568-76. doi: 10.1101/gr.129684.111. PubMed
984 PMID: 22300766.
985
986
987
988
989
990
991
992
993
994
995
996
997
998
999
1000

bioRxiv preprint doi: https://doi.org/10.1101/2021.04.09.439146; this version posted April 9, 2021. The copyright holder for this preprint (which was not certified by peer review) is the author/funder, who has granted bioRxiv a license to display the preprint in perpetuity. It is made available under aCC-BY 4.0 International license.

FIGURE CAPTIONS

Fig 1. Experimental design of the *in vitro* generation of genetic variability studies for HSV-1 and HSV-2 subtypes and detected changes in plaque phenotype. (A) Five viral clones from each original stock were five times plaque-purified in Vero cells and then deep sequenced. Two clones were re-sequenced at ultrahigh depth, whose replication, infectivity, and pathogenesis were compared to their corresponding parental stocks in cell culture and animal models of infection (S4 Fig). Those two clones were used to infect Vero and HaCaT cells at an MOI of 0.1 PFU/cell. After 48 hpi, viral progenies were harvested, referring to this infection cycle as a passage. Viral populations from each plaque-purified clone were ultra-deep sequenced after five and ten passages in each cell line. (B) Four representative pictures are showing the plaque morphology phenotype of HSV-1 clone 3 in Vero cells (48 hpi), before (passage 0, P0), and after ten passages (P10) in Vero cells. This syncytial plaque phenotype is due to the previously well-described syncytia-inducing mutation in UL27 CDS (see S9 Table, variant #38: R858H) [37]. Tiled images (4 x 4) were taken using a Leica DM IL LED inverted microscope equipped with a Leica DFC3000-G digital camera. Scale bars indicate 100 μm.

Fig 2. Genetic diversity in viral populations from original stocks and five times plaque-isolated HSV-1 and HSV-2 clones. (A) Total number of MVs observed in each original stock, at a frequency equals or above a 1% limit of detection (see Materials and Methods for details). The total number of MVs (*y*-axis) is separated into variant type and genomic location (*x*-axis). Variant type distinguishes between SNPs and InDels, discriminating nonsynonymous SNPs. The genomic location of each variant is categorized as non-coding or coding region. (B) Histograms show the number of MVs in each frequency range for each original stock. The frequency of each variant was examined and grouped in shown ranges (e.g., 10% to <20% frequency, 20% to <30%

bioRxiv preprint doi: https://doi.org/10.1101/2021.04.09.439146; this version posted April 9, 2021. The copyright holder for this preprint (which was not certified by peer review) is the author/funder, who has granted bioRxiv a license to display the preprint in perpetuity. It is made available under aCC-BY 4.0 International license.

1029 frequency and so on). SNPs and InDels were combined for this analysis. (C) Total
1030 number of MVs observed in each HSV-1 (left, blue bars) and HSV-2 (right, red bars)
1031 clones after five rounds of plaque-isolation, categorized by nonconservative changes
1032 (SNPs and InDels). See S3 and S4 Tables for a full list of MVs position and frequency
1033 data. (D) Total number of variants detected in each clone are grouped by subtype and
1034 graphed showing mean +/- SEM (ns = not significant $p > 0.05$ by two-tailed Mann–
1035 Whitney *U*-test).
1036
1037 **Fig 3. Comparative variant analysis from standard- and ultra-deep sequencing**
1038 **data of two plaque-isolated HSV-1 and HSV-2 clones.** (A) Histograms show the
1039 average depth of coverage per genomic position of reads alignments from standard-
1040 deep sequencing (SDS, white bars) and ultra-deep sequencing (UDS, black bars) for
1041 each viral clone. (B) Histograms bar plot total number of MVs observed after variant
1042 analysis of SDS and UDS data in each viral clone, discriminating between preexisting
1043 MVs found in the corresponding original stock (white) and *de novo* appearance (red).
1044 (C) The number of total, preexisting, and *de novo* MVs detected in each clone from
1045 SDS, and UDS data are grouped and graphed (blue shapes for HSV-1, red for HSV-2
1046 clones), showing mean +/- SEM (ns $p > 0.05$, * $p = 0.029$ by two-tailed Mann–Whitney
1047 *U*-test). (D) Number of *de novo* MVs observed after variant analysis of SDS and UDS
1048 data in each viral clone, stacked by frequency ranges. SNPs and InDels were
1049 combined for this analysis. (E) *de novo* MVs with a frequency between 1% to 2%
1050 detected in each clone from SDS, and UDS data are grouped and graphed (blue
1051 shapes for HSV-1, red for HSV-2 clones), showing mean +/- SEM (* $p = 0.029$ by two-
1052 tailed Mann–Whitney *U*-test). See S5 and S6 Tables for a full list of MVs position and
1053 frequency data.
1054
1055 **Fig 4. Comparison of *de novo* generation of total and nonconservative genetic**
1056 **diversity between HSV-1 and HSV-2 purified clones, after five (P5) and ten (P10)**

bioRxiv preprint doi: https://doi.org/10.1101/2021.04.09.439146; this version posted April 9, 2021. The copyright holder for this preprint (which was not certified by peer review) is the author/funder, who has granted bioRxiv a license to display the preprint in perpetuity. It is made available under aCC-BY 4.0 International license.

passages in Vero and HaCaT cells. (A) Total number of MVs are plotted according to variant analysis data for each clone, passage, and cell line, differentiating between preexisting MVs observed in the corresponding passage zero (P0) in white, and *de novo* generated MVs in red. (B) Number of *de novo* SNPs detected in each viral population, categorized by nonsynonymous (black) and synonymous/non-coding changes (white). (C) Number of de novo InDels detected among each viral population are stacked by their location impacting coding regions (black) or non-coding regions (white). (D) *De novo* MVs are stacked by frequency ranges. SNPs and InDels were combined for this analysis. See S7-S14 Tables for a full list of MVs position and frequency data.

Fig 5. Stacked histograms show the number of *de novo* genic MVs (*x*-axis) located in each HSV-1 (left) and HSV-2 (right) coding sequence (gene; *y*-axis), after five (P5) and ten (P10) passages in Vero and HaCaT cells. Only coding sequences registering at least one variant are included in the histogram. MVs found in both copies of each RL1, RL2, and RS1 coding sequences are listed together. SNPs and InDels were combined for this analysis. See S7-S14 Tables for a full list of MVs position and frequency data.

Fig 6. Dynamics of nonconservative *de novo* variants in each HSV-1 (left) and HSV-2 purified populations (right), whose frequency increased over sequential passages in cell culture. Nonsynonymous *de novo* SNPs were plotted by their frequency in the sequenced viral population after five (P5) and ten (P10) passages in Vero and HaCaT cells. SNPs, their encoded proteins (bold), as well as the change that they would cause in the translated protein (italic), are listed in the legend according to their frequency at P5 and P10.

bioRxiv preprint doi: https://doi.org/10.1101/2021.04.09.439146; this version posted April 9, 2021. The copyright holder for this preprint (which was not certified by peer review) is the author/funder, who has granted bioRxiv a license to display the preprint in perpetuity. It is made available under aCC-BY 4.0 International license.

SUPPORTING INFORMATION CAPTIONS

S1 Fig. Schematic of the HSV-1 strain SC16 (A) and HSV-2 strain 333 (B) sequenced genomes from original stocks. Each CDS is presented in forward (red) or reverse (blue) orientation. Detected MVs are mapped as black (not *de novo*) or red (*de novo*) dots across the genome, according to their location (*x*-axis) and frequency (*y*-axis). GC% plots (purple lines) and coverage plots from data alignments (blue/orange profiles) have also been mapped across each genome.

S2 Fig. Variant analysis of HSV-1 plaque-purified clones. Coverage plots from data alignments are represented in blue, for each individual case. Detected MVs are mapped as black (not *de novo*) or red (*de novo*) dots across the genome, according to their location (*x*-axis) and frequency (*y*-axis). MVs were considered as *de novo* when these were not previously found in the original stock (see Materials and Methods for details).

S3 Fig. Variant analysis of HSV-2 plaque-purified clones. Coverage plots from data alignments are represented in orange, for each individual case. Detected MVs are mapped as black (not *de novo*) or red (*de novo*) dots across the genome, according to their location (*x*-axis) and frequency (*y*-axis). MVs were considered as *de novo* when these were not previously found in the original stock.

S4 Fig. Replication kinetics and pathogenesis of HSV-1 and HSV-2 plaque-isolated clones compared to their corresponding original stocks. (A) Vero cells were infected with the indicated viruses at high MOI (5 PFU/cell) for one-step growth curves, and at low MOI (0.01 PFU/cell) for multi-step growth curves. Virus titers from fractions containing cell-associated virus were determined by plaque assay at 24 hpi in the one-step curves, and at the indicated times in the multi-step curves. (B) Female

bioRxiv preprint doi: https://doi.org/10.1101/2021.04.09.439146; this version posted April 9, 2021. The copyright holder for this preprint (which was not certified by peer review) is the author/funder, who has granted bioRxiv a license to display the preprint in perpetuity. It is made available under aCC-BY 4.0 International license.

BALB/c mice (n=5) were infected with the indicated virus and dose, by intranasal (i.n.) or intravaginal (i.v.) inoculations. Mice were monitored daily for survival, body weight, and signs of illness. Weight data are expressed as the mean +/- SEM of the five animal weights compared to their original weight on the day of inoculation. Signs of illness, as a score ranged from 1 to 4, is also expressed as the mean +/- SEM of the five animals. A colored "1" indicates thereafter only one animal remained in that group. Statistical analysis was performed for bodyweight data, using multiple *t*-tests with Sidak-Bonferroni correction ($p < 0.05$).

S5 Fig. Variant analysis of HSV-1 plaque-purified clones 2 and 3 (A) and HSV-2 clones 1 and 5 (B) from high-depth sequencing data. Coverage plots from alignments are represented in blue or orange, for each case. Detected MVs are mapped as black (not *de novo*) or red (*de novo*) dots across the genome, according to their location (*x*-axis) and frequency (*y*-axis). MVs were considered as *de novo* when these were not previously found in the corresponding original stock.

S6 Fig. Variant analysis of HSV-1 plaque-purified clone 2, after 5 and 10 passages in Vero and HaCaT cells. Coverage plots from high-depth sequencing data alignments are represented in blue. Detected MVs are mapped as black (not *de novo*) or red (*de novo*) dots across the genome, according to their location (*x*-axis) and frequency (*y*-axis). Mutations from passage 0 were considered as *de novo* when these were not previously found in the original stock, whereas those from passage 5 and 10, regarding passage 0.

S7 Fig. Variant analysis of HSV-1 plaque-purified clone 3, after 5 and 10 passages in Vero and HaCaT cells. Coverage plots from high-depth sequencing data alignments are represented in blue. Detected MVs are mapped as black (not *de novo*) or red (*de novo*) dots across the genome, according to their location (*x*-axis) and

bioRxiv preprint doi: https://doi.org/10.1101/2021.04.09.439146; this version posted April 9, 2021. The copyright holder for this preprint (which was not certified by peer review) is the author/funder, who has granted bioRxiv a license to display the preprint in perpetuity. It is made available under aCC-BY 4.0 International license.

frequency (*y*-axis). Mutations from passage 0 were considered as *de novo* when these were not previously found in the original stock, whereas those from passage 5 and 10, regarding passage 0.

S8 Fig. Variant analysis of HSV-2 plaque-purified clone 1, after 5 and 10 passages in Vero and HaCaT cells. Coverage plots from high-depth sequencing data alignments are represented in orange. Detected MVs are mapped as black (not *de novo*) or red (*de novo*) dots across the genome, according to their location (*x*-axis) and frequency (*y*-axis). Mutations from passage 0 were considered as *de novo* when these were not previously found in the original stock, whereas those from passage 5 and 10, regarding passage 0.

S9 Fig. Variant analysis of HSV-2 plaque-purified clone 5, after 5 and 10 passages in Vero and HaCaT cells. Coverage plots from high-depth sequencing data alignments are represented in orange. Detected MVs are mapped as black (not *de novo*) or red (*de novo*) dots across the genome, according to their location (*x*-axis) and frequency (*y*-axis). Mutations from passage 0 were considered as *de novo* when these were not previously found in the original stock, whereas those from passage 5 and 10, regarding passage 0.

S1 Animation. Variant analysis of HSV-1 plaque-purified clone 2, after 5 and 10 passages in Vero and HaCaT cells. See S5 Fig for additional details.

S2 Animation. Variant analysis of HSV-1 plaque-purified clone 3, after 5 and 10 passages in Vero and HaCaT cells. See S6 Fig for additional details.

S3 Animation. Variant analysis of HSV-2 plaque-purified clone 1, after 5 and 10 passages in Vero and HaCaT cells. See S7 Fig for additional details.

bioRxiv preprint doi: https://doi.org/10.1101/2021.04.09.439146; this version posted April 9, 2021. The copyright holder for this preprint (which was not certified by peer review) is the author/funder, who has granted bioRxiv a license to display the preprint in perpetuity. It is made available under aCC-BY 4.0 International license.

S4 Animation. Variant analysis of HSV-2 plaque-purified clone 5, after 5 and 10 passages in Vero and HaCaT cells. See S8 Fig for additional details.

S1 Table. Genome sequencing statistics for each sample sequenced in this study.

Legend: SRA (Sequence Read Archive), QF (quality-filtered).

S2 Table. Categorized number of MVs for each sample sequenced in this study.

Legend: NCR (non-coding region), CR (coding region).

S3 Table. List of detected MVs from deep sequencing of HSV-1 original stock and plaque-purified clones 1-5.

Legend: Ref (reference allele), Var (variant allele), NCR (non-coding region), INS (insertion), DEL (deletion), *name*_freq (variant allele frequency), *name*_cov (total coverage), *name*_Ref (reference allele coverage), *name*_Var (variant allele coverage).

S4 Table. List of detected MVs from deep sequencing of HSV-2 original stock and plaque-purified clones 1-5.

Legend: Ref (reference allele), Var (variant allele), NCR (non-coding region), INS (insertion), DEL (deletion), *name*_freq (variant allele frequency), *name*_cov (total coverage), *name*_Ref (reference allele coverage), *name*_Var (variant allele coverage).

S5 Table. List of detected MVs from ultra-deep sequencing of HSV-1 plaque-purified clones 2 and 3.

Legend: Ref (reference allele), Var (variant allele), NCR (non-coding region), INS (insertion), DEL (deletion), *name*_freq (variant allele frequency), *name*_cov (total coverage), *name*_Ref (reference allele coverage), *name*_Var (variant allele coverage).

bioRxiv preprint doi: https://doi.org/10.1101/2021.04.09.439146; this version posted April 9, 2021. The copyright holder for this preprint (which was not certified by peer review) is the author/funder, who has granted bioRxiv a license to display the preprint in perpetuity. It is made available under aCC-BY 4.0 International license.

S6 Table. List of detected MVs from ultra-deep sequencing of HSV-2 plaque-purified clones 1 and 5.

Legend: Ref (reference allele), Var (variant allele), NCR (non-coding region), INS (insertion), DEL (deletion), *name*_freq (variant allele frequency), *name*_cov (total coverage), *name*_Ref (reference allele coverage), *name*_Var (variant allele coverage).

S7 Table. List of detected MVs from ultra-deep sequencing of HSV-1 clone 2 at P0, P5, and P10 in Vero cells.

Legend: Ref (reference allele), Var (variant allele), NCR (non-coding region), INS (insertion), DEL (deletion), *name*_freq (variant allele frequency), *name*_cov (total coverage), *name*_Ref (reference allele coverage), *name*_Var (variant allele coverage).

S8 Table. List of detected MVs from ultra-deep sequencing of HSV-1 clone 2 at P0 in Vero cells, and P5 and P10 in HaCaT cells.

Legend: Ref (reference allele), Var (variant allele), NCR (non-coding region), INS (insertion), DEL (deletion), *name*_freq (variant allele frequency), *name*_cov (total coverage), *name*_Ref (reference allele coverage), *name*_Var (variant allele coverage).

S9 Table. List of detected MVs from ultra-deep sequencing of HSV-1 clone 3 at P0, P5, and P10 in Vero cells.

Legend: Ref (reference allele), Var (variant allele), NCR (non-coding region), INS (insertion), DEL (deletion), *name*_freq (variant allele frequency), *name*_cov (total coverage), *name*_Ref (reference allele coverage), *name*_Var (variant allele coverage).

S10 Table. List of detected MVs from ultra-deep sequencing of HSV-1 clone 3 at P0 in Vero cells, and P5 and P10 in HaCaT cells.

bioRxiv preprint doi: https://doi.org/10.1101/2021.04.09.439146; this version posted April 9, 2021. The copyright holder for this preprint (which was not certified by peer review) is the author/funder, who has granted bioRxiv a license to display the preprint in perpetuity. It is made available under aCC-BY 4.0 International license.

Legend: Ref (reference allele), Var (variant allele), NCR (non-coding region), INS (insertion), DEL (deletion), *name*_freq (variant allele frequency), *name*_cov (total coverage), *name*_Ref (reference allele coverage), *name*_Var (variant allele coverage).

S11 Table. List of detected MVs from ultra-deep sequencing of HSV-2 clone 1 at P0, P5, and P10 in Vero cells.

Legend: Ref (reference allele), Var (variant allele), NCR (non-coding region), INS (insertion), DEL (deletion), *name*_freq (variant allele frequency), *name*_cov (total coverage), *name*_Ref (reference allele coverage), *name*_Var (variant allele coverage).

S12 Table. List of detected MVs from ultra-deep sequencing of HSV-2 clone 1 at P0 in Vero cells, and P5 and P10 in HaCaT cells.

Legend: Ref (reference allele), Var (variant allele), NCR (non-coding region), INS (insertion), DEL (deletion), *name*_freq (variant allele frequency), *name*_cov (total coverage), *name*_Ref (reference allele coverage), *name*_Var (variant allele coverage).

S13 Table. List of detected MVs from ultra-deep sequencing of HSV-2 clone 5 at P0, P5, and P10 in Vero cells.

Legend: Ref (reference allele), Var (variant allele), NCR (non-coding region), INS (insertion), DEL (deletion), *name*_freq (variant allele frequency), *name*_cov (total coverage), *name*_Ref (reference allele coverage), *name*_Var (variant allele coverage).

S14 Table. List of detected MVs from ultra-deep sequencing of HSV-2 clone 5 at P0 in Vero cells, and P5 and P10 in HaCaT cells.

Legend: Ref (reference allele), Var (variant allele), NCR (non-coding region), INS (insertion), DEL (deletion), *name*_freq (variant allele frequency), *name*_cov (total coverage), *name*_Ref (reference allele coverage), *name*_Var (variant allele coverage).

bioRxiv preprint doi: https://doi.org/10.1101/2021.04.09.439146; this version posted April 9, 2021. The copyright holder for this preprint (which was not certified by peer review) is the author/funder, who has granted bioRxiv a license to display the preprint in perpetuity. It is made available under aCC-BY 4.0 International license.

S1 Text. Supporting Material and Methods for HSV replication kinetics and infection models shown in S4 Fig.

Virus growth curves protocol, ethical statement, description of procedures employed to infect and monitor mouse pathogenesis, and statistical analysis.

bioRxiv preprint doi: https://doi.org/10.1101/2021.04.09.439146; this version posted April 9, 2021. The copyright holder for this preprint (which was not certified by peer review) is the author/funder, who has granted bioRxiv a license to display the preprint in perpetuity. It is made available under aCC-BY 4.0 International license.

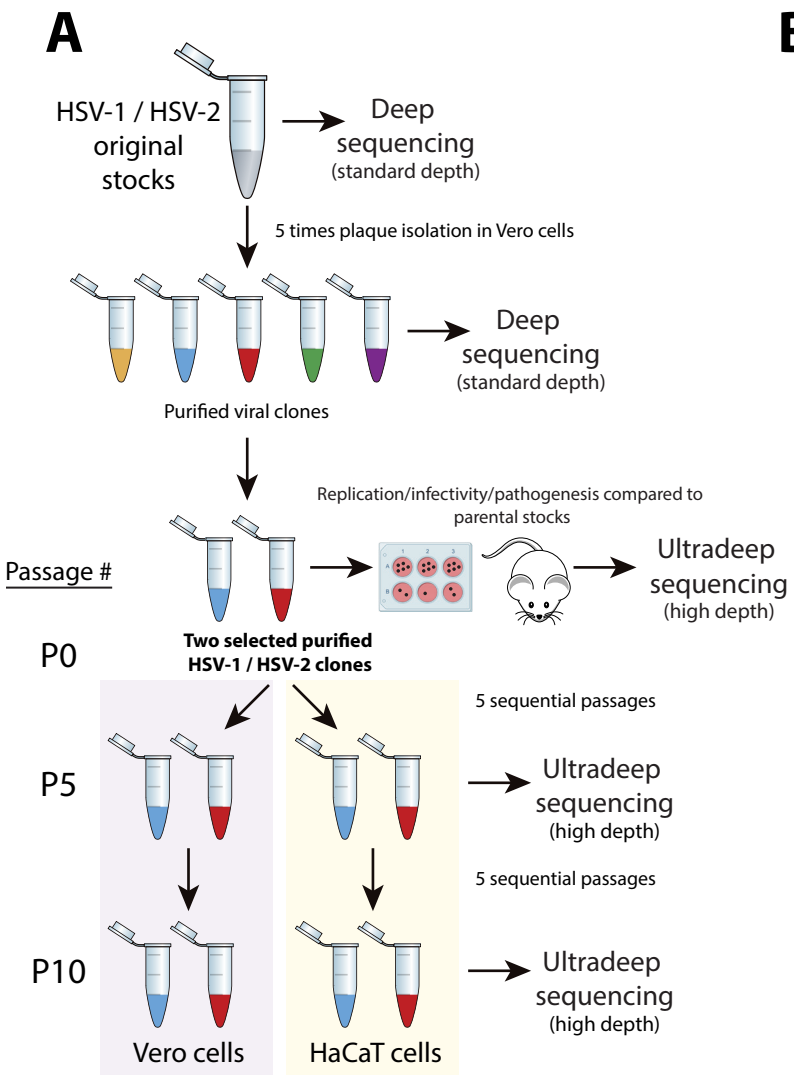

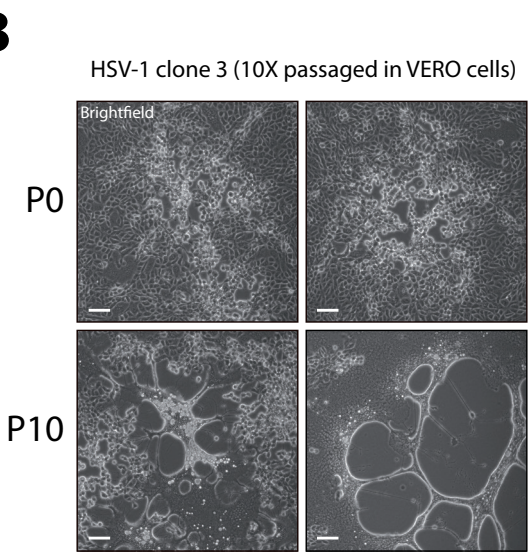

Fig 1

bioRxiv preprint doi: https://doi.org/10.1101/2021.04.09.439146; this version posted April 9, 2021. The copyright holder for this preprint (which was not certified by peer review) is the author/funder, who has granted bioRxiv a license to display the preprint in perpetuity. It is made available under aCC-BY 4.0 International license.

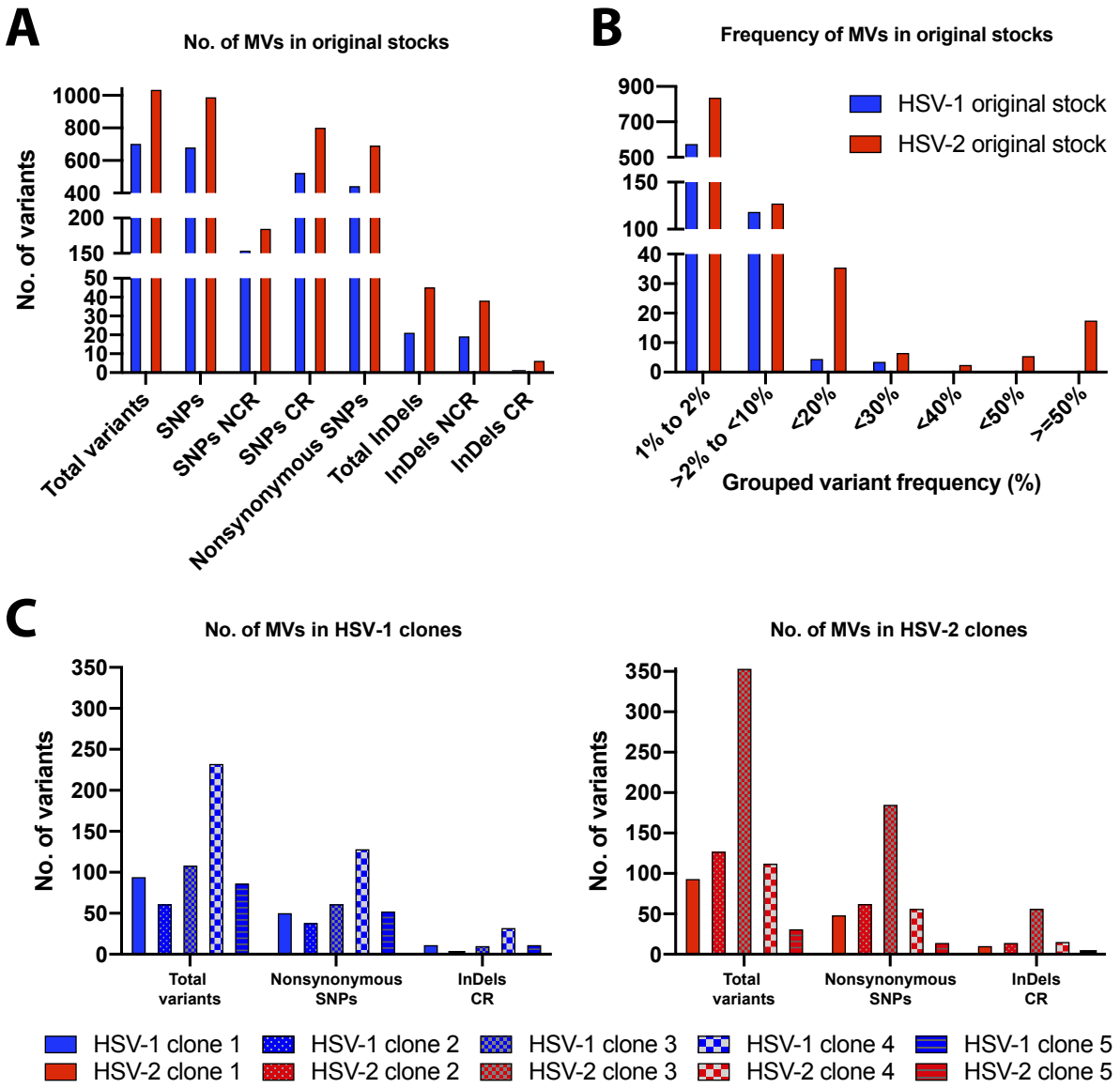

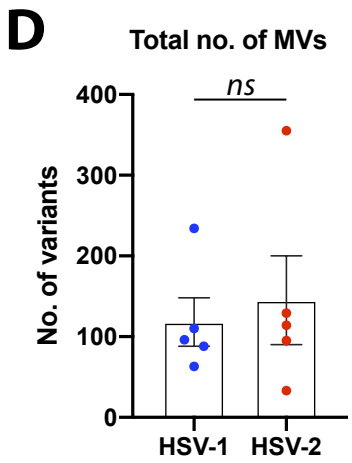

Fig 2

bioRxiv preprint doi: https://doi.org/10.1101/2021.04.09.439146; this version posted April 9, 2021. The copyright holder for this preprint (which was not certified by peer review) is the author/funder, who has granted bioRxiv a license to display the preprint in perpetuity. It is made available under aCC-BY 4.0 International license.

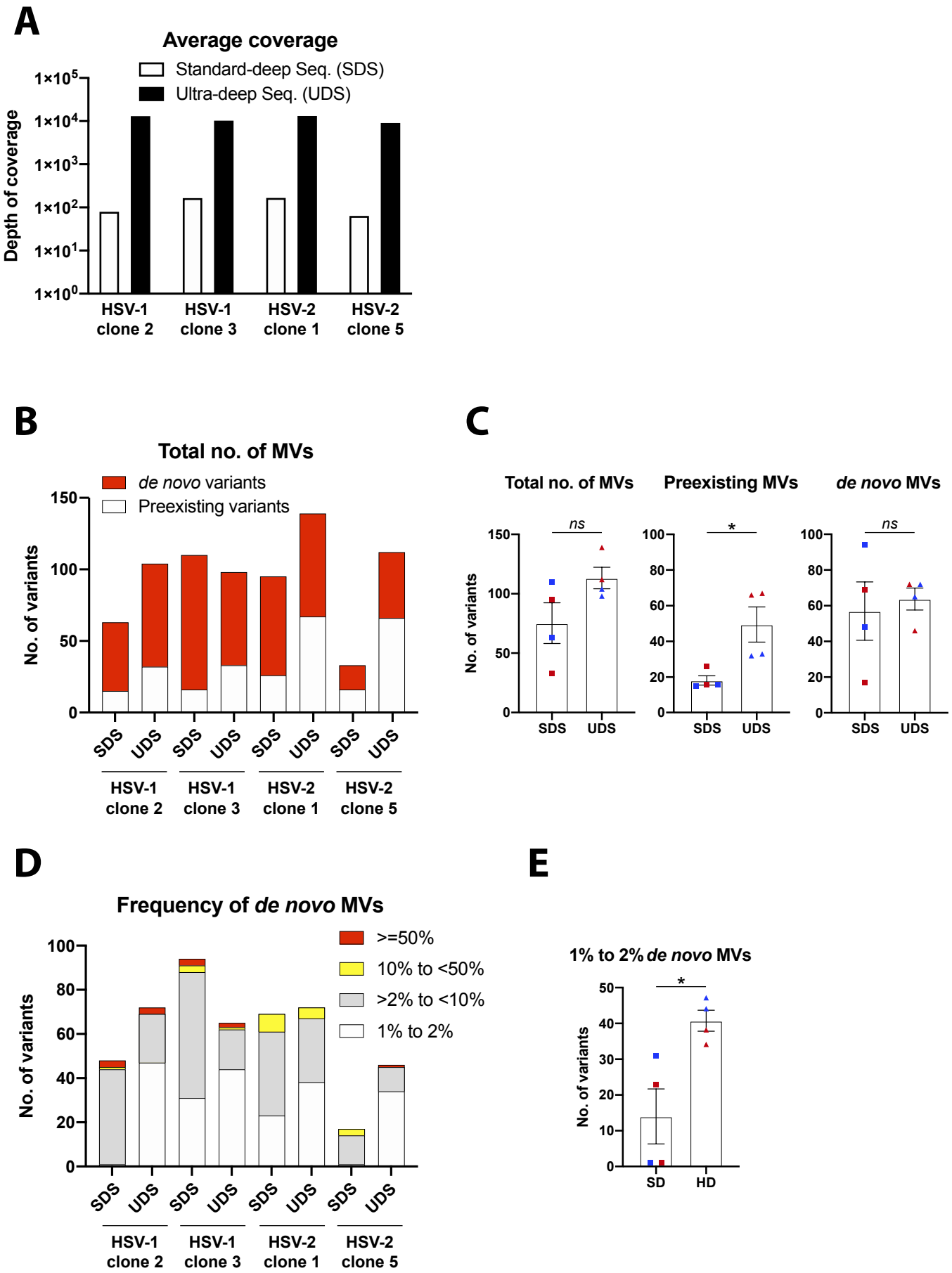

Fig 3

bioRxiv preprint doi: https://doi.org/10.1101/2021.04.09.439146; this version posted April 9, 2021. The copyright holder for this preprint (which was not certified by peer review) is the author/funder, who has granted bioRxiv a license to display the preprint in perpetuity. It is made available under aCC-BY 4.0 International license.

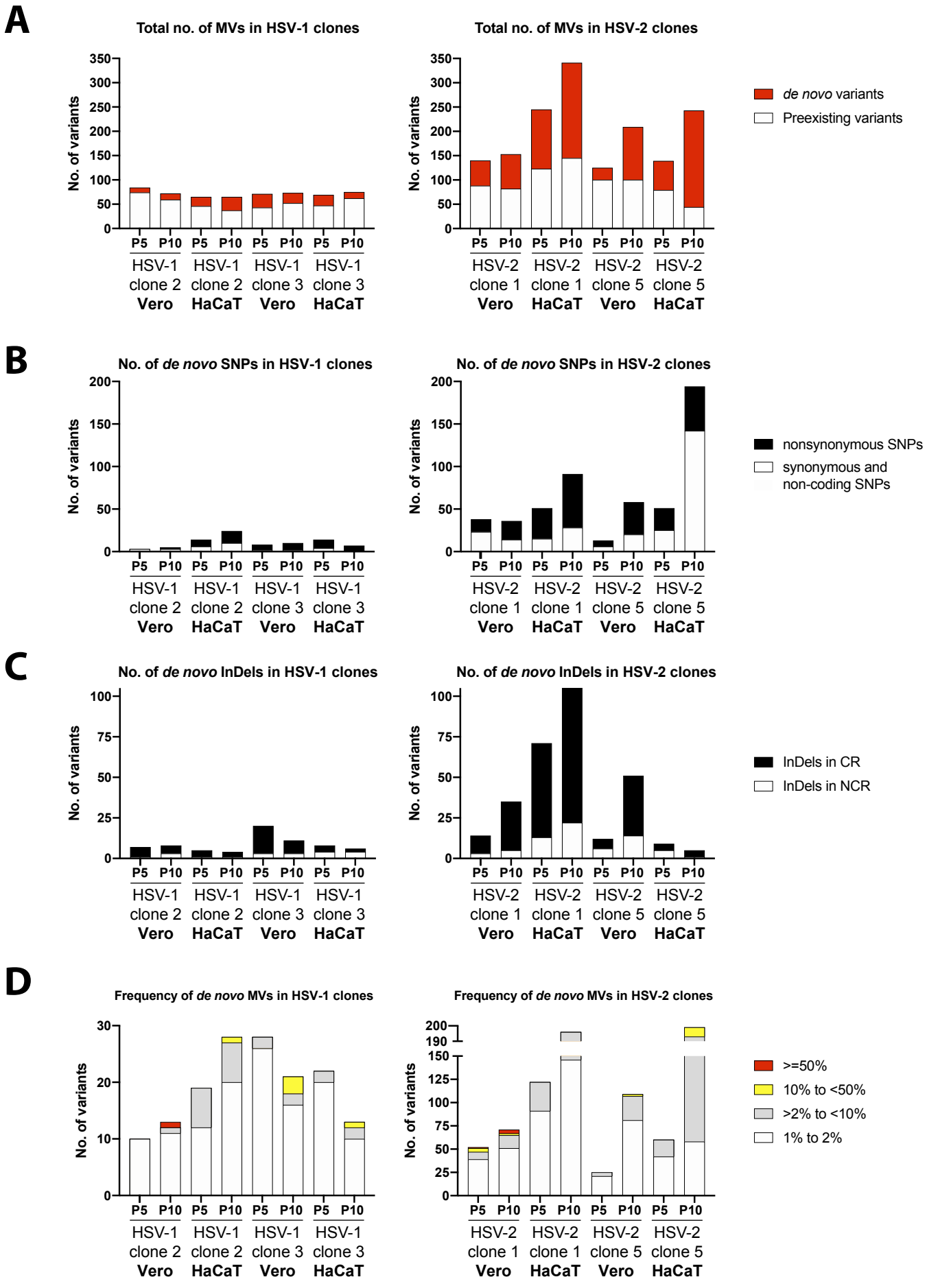

Fig 4

bioRxiv preprint doi: https://doi.org/10.1101/2021.04.09.439146; this version posted April 9, 2021. The copyright holder for this preprint (which was not certified by peer review) is the author/funder, who has granted bioRxiv a license to display the preprint in perpetuity. It is made available under aCC-BY 4.0 International license.

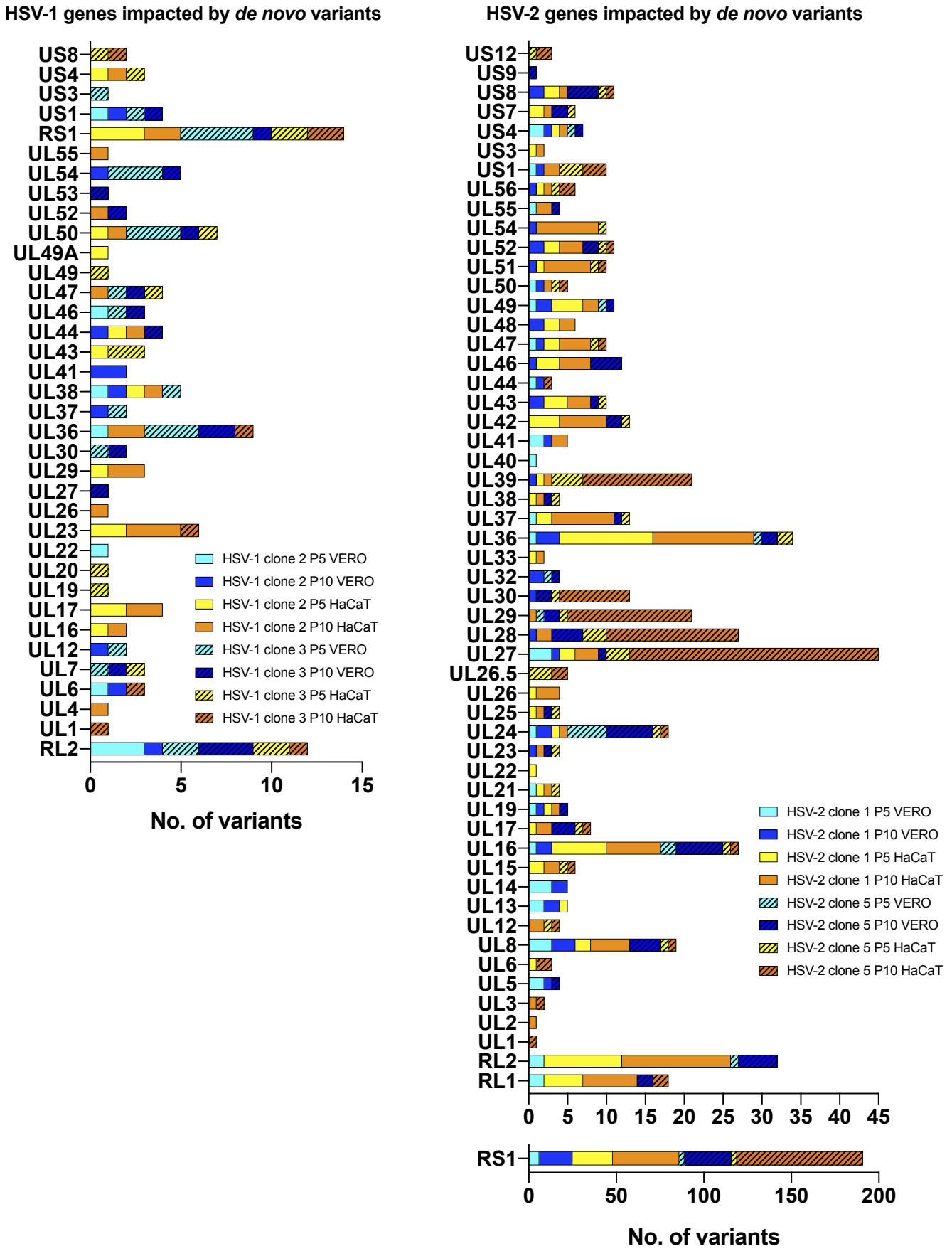

Fig 5

bioRxiv preprint doi: https://doi.org/10.1101/2021.04.09.439146; this version posted April 9, 2021. The copyright holder for this preprint (which was not certified by peer review) is the author/funder, who has granted bioRxiv a license to display the preprint in perpetuity. It is made available under aCC-BY 4.0 International license.

Nonsynonymous *de novo* SNPs that increase in frequency in HSV-1

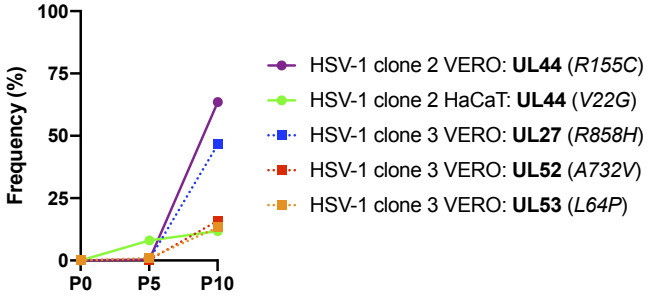

Nonsynonymous *de novo* SNPs that increase in frequency in HSV-2

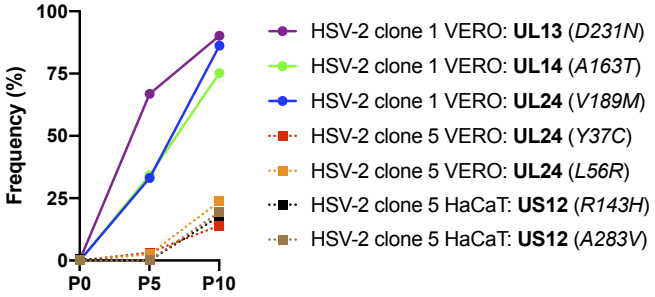

Fig 6